

IRIA

CENTRE

SOPHIA ANTIPOLIS

Institut National
de Recherche
en Informatique
et en Automatique

Domaine de Voluceau
Rocquencourt
BP 105

78153 Le Chesnay Cedex
France

Tel (3) 954 9020

Rapports de Recherche

N° 420

AN OPTIMAL TRIANGULATION FOR SECOND ORDER ELLIPTIC PROBLEMS

Michel DELFOUR
Guy PAYRE
Jean-Paul ZOLÉSIO

Juillet 1985

AN OPTIMAL TRIANGULATION FOR SECOND ORDER
ELLIPTIC PROBLEMS¹

Michel M. Delfour², G. Payre³, and J.-P. Zolésio⁴

December 1984

CRMA-1203

1. This research was supported in part by the National Sciences and Engineering Council Canada Grant A-8730 and a "Subvention FCAC du Ministère de l'Éducation du Québec".
2. Centre de Mathématiques Appliquées, Ecole Nationale Supérieure des Mines de Paris, and INRIA, Sophia Antipolis 06560 - Valbonne, France (Permanent address: Centre de recherche de mathématiques appliquées, Université de Montréal, C.P.6128, Succ.A, Montréal, Québec, Canada H3C 3J7.
3. Département de génie mécanique, Université de Sherbrooke, Sherbrooke, Québec, Canada J1K 2R1.
4. Département de mathématiques, Université de Nice, 06034 Nice, Cedex, France.

Résumé. Soit Ω un domaine polygonal dans \mathbb{R}^n , \mathcal{T}_h une triangularisation de Ω et u_h la "solution éléments finis" d'un problème elliptique du deuxième ordre sur (Ω, \mathcal{T}_h) . Soit $M = \{M_i : 1 \leq i \leq p+q\}$ l'ensemble des noeuds qui définissent les sommets de la triangularisation \mathcal{T}_h : pour chaque i , $M_i = (x_i^1, \dots, x_i^n)$ (que l'on note $M_i = (x_i^\ell)$, $1, \leq \ell \leq n$).

L'objectif de cet article est de fournir un outil de calcul pour approcher de l'ensemble des meilleures positions \hat{M} des noeuds et essayer d'obtenir la meilleure triangularisation $\hat{\mathcal{T}}_h$ qui minimise l'erreur entre la solution approchée u_h et la vraie solution u dans la norme naturelle associée à ce problème.

L'essentiel de cet article consiste en deux théorèmes qui donnent des expressions explicites pour les dérivées partielles des fonctionnelles d'énergie par rapport aux coordonnées x_i^ℓ de chaque noeud variable M_i , $1 \leq i \leq p$.



ABSTRACT

Let Ω be a polygonal domain in R^n , τ_h an associated triangulation and u_h the finite element solution of a well-posed second order elliptic problem on (Ω, τ_h) . Let $M = \{M_i\}_{i=1}^{p+q}$ be the set of nodes which defines the vertices of the triangulation τ_h : for each i , $M_i = (x_i^\ell | 1 \leq \ell \leq n)$ in R^n . The object of this paper is to provide a computational tool to approximate the best set of positions \hat{M} of the nodes and hence the best triangulation $\hat{\tau}_h$ which minimizes the solution error in the natural norm associated with the problem.

The main result of this paper are theorems which provide explicit expressions for the partial derivatives of the associated energy functional with respect to the coordinates x_i^ℓ , $1 \leq \ell \leq n$ of each of the variable node M_i , $i=1, \dots, p$.

1. INTRODUCTION

The object of this paper is the optimal triangular meshing for a large class of linear second order elliptic problems. Its mathematical formulation is equivalent to the minimization of the solution error with respect to the positions of the nodes. The boundary nodes at the vertices of the polygonal domain are assumed to be fixed in position and number; the other nodes are free but their total number is fixed. A complete mathematical analysis is presented which does not involve ad hoc considerations (numerical or physical).

Explicit expressions for the directional gradient of the solution error with respect to the position of the variable nodes are given. They turn out to be independent of the exact solution of the linear elliptic boundary value problem. Moreover gradient computations are easily implementable within a finite element code. In fact gradient computations can be done in parallel with the computation of the solution.

The finite element triangular meshing optimization has been recently addressed by a number of authors (cf. Liniecki and Yun [1], W.C. Tacker [1], Shephard and Gallagher [1], McNeice and Marcal [1], Melosh and Marcal [1], Shephard, Gallagher and Abel [1], Seguchi, Tomita and Hashimoto [1], Bardfield [1]). The reader is referred to the first paper for a discussion of the literature. For instance, our analysis applies to the torsion problem considered by Liniecki and Yun [1]. However our choice of optimization criterion is different and, in our mind, mathematically and computationally simpler.

The optimization of the triangulation is an important problem in itself. But it is of paramount importance in the shape optimization problem when the nodes are chosen as design parameters.

Since, in general, the number of nodes is large, it is customary to introduce a reduced number of control parameters which will effectively control the positions of the nodes. An optimal triangulation can also be obtained within this class of controlled triangulations by using our analysis combined with a straightforward application of the chain rule.

The ideas and techniques used in this paper are based on an adaptation of the "speed method" to finite element approximations (cf. J.P. Zolésio [1,2]).

Notation.

\mathbb{R} is the field of all real numbers and \mathbb{R}^n the Euclidean n -dimensional space. Given a domain Ω in \mathbb{R}^n , $\bar{\Omega}$ denotes the closure of Ω and $H^m(\Omega)$, $m \geq 1$ an integer, the Sobolev space of square integrable function from Ω to \mathbb{R} with square integrable partial derivatives up to order m (in the distribution sense). Let Γ be the boundary of the domain Ω . $H_0^1(\Omega)$ will be the subspace of functions of $H^1(\Omega)$ which are zero on the boundary Γ . By interpolation theory it is possible to define Sobolev spaces with fractional power such as $H^{\frac{1}{2}}(\Gamma)$. In particular the trace of a function v in $H^1(\Omega)$ on the boundary Γ belongs to $H^{\frac{1}{2}}(\Gamma)$. The topological dual of $H^{\frac{1}{2}}(\Gamma)$ will be denoted $H^{-\frac{1}{2}}(\Gamma)$. For more details the reader is referred to Ph. Ciarlet [1].

We shall often use the notation $f \circ T$ for the composition of a function $f: \mathbb{R}^n \rightarrow \mathbb{R}$ with a transformation $T: \mathbb{R}^n \rightarrow \mathbb{R}^n$

$$\forall x \in \mathbb{R}^n \quad (f \circ T) = f(T(x)).$$

2. PROBLEM FORMULATION

It is well-known that large families of linear elliptic boundary-value problems can be transformed into variational problems of the following form (cf. Ph.G. Ciarlet [1]). Let V be a Hilbert space (e.g. a closed subspace of the Sobolev space $H^1(\Omega)$) and u be the solution of the variational problem

$$(1) \quad u \in V, \quad \forall \varphi \in V, \quad a(u, \varphi) = \langle F, \varphi \rangle_V$$

where $\langle \cdot, \cdot \rangle_V$ is the duality pairing between V' and V , F is a fixed element of V' and a is a coercive continuous bilinear form on V

$$(2) \quad \exists \alpha > 0, \quad \forall v \in V, \quad a(v, v) \geq \alpha \|v\|_V^2$$

and $\| \cdot \|$ is the norm in V . Under the above hypothesis $\sqrt{a(v, v)}$ is a norm which is equivalent to $\|v\|$ on V . In general the bilinear form a need not be symmetrical.

Let V_h be a finite dimensional subspace of V and let u_h be the solution of the variational problem

$$(1_h) \quad u_h \in V_h, \quad \forall v_h \in V_h, \quad a(u_h, v_h) = \langle F, v_h \rangle_V.$$

For instance V can be a closed subspace of the Sobolev space $H^1(\Omega)$ and Ω a polygonal domain in \mathbb{R}^n . If τ_h denotes a triangulation of Ω , V_h can be chosen in the following way

$$(3) \quad V_h = \{v_h \in V \mid v_h|_K \in P^k(K), \quad \forall K \in \tau_h\}$$

where $P^k(K)$ is the space of polynomials of order less or equal to $k \geq 1$ on the triangle K .

The standard theory (cf. J. Céa [1]) indicates that the solution error is bounded by the interpolation error

$$(4) \quad \|u - u_h\|_V \leq Cd(u, V_h)$$

where $d(u, V_h)$ is the minimum distance of the solution u to the subspace V_h of V measured in the V -norm and $C > 0$ is a constant which does not depend on u and V_h .

From now on we specialize to the case where V is a closed subspace of $H^1(\Omega)$, V_h is given by (3), that is, linear elliptic second order problems. When the solution u to equation (1) is sufficiently smooth it can be shown (cf. Ph.G. Ciarlet [1]) that

$$(5) \quad d(u, V_h) \leq c(u)h^k$$

where h is the "size" of the triangulation and $c(u)$ is a constant which depends on u but not on the choice of the triangulation τ_h . The final upper bound

$$(6) \quad \|u - u_h\|_V \leq c(u)h^k$$

provided in the finite element method is established for all left-hand-sides F in V' . Indeed $c(u)$ has an upper bound $c_1(F, \Omega)$ which solely depends on F and Ω (but not on the triangulation τ_h).

3. FORMULATION OF THE OPTIMAL TRIANGULATION PROBLEM

Let Ω be a polygonal domain and τ_h its triangulation. Denote by

$$\bar{M} = \{M_i \mid 1 \leq i \leq p+q\}, \quad p \geq 1, \quad q \geq 2,$$

(p and q integers) the set of all nodes in the triangulation of the domain $\bar{\Omega}$, by

$$\partial M = \{M_i \mid p+1 \leq i \leq p+q\}$$

the set of all vertices of Ω on the boundary $\partial\Omega$ and by M

$$M = \{M_i \in \bar{M} \mid M_i \notin \partial M\} = \{M_i \mid 1 \leq i \leq p\}$$

the set of all nodes which are not vertices on $\partial\Omega$.

Our objective is to construct a triangulation τ'_h of Ω by moving the p variable nodes $M = \{M_i\}_{i=1}^p$ in such a way that the resulting error $\|u - u'_h\|$ be smaller than the initial error $\|u - u_h\|$ for the triangulation τ_h . We assume that the number and the position of the nodes at the vertices are fixed.

The solutions u and u_h to problems (1) and (1_h) coincide with the minimizing elements of the problems

$$(7) \quad \text{Inf}\{J(\varphi) : \varphi \in V\}$$

$$(7_h) \quad \text{Inf}\{J(\varphi_h) : \varphi_h \in V_h\},$$

where

$$(8) \quad J(\varphi) = \frac{1}{2}a(\varphi, \varphi) - \langle F, \varphi \rangle$$

The directional derivatives of J are given by

$$(9) \quad dJ(\varphi; \psi) = \frac{1}{2}[a(\varphi, \psi) + a(\psi, \varphi)] - \langle F, \psi \rangle$$

$$(10) \quad d^2J(\varphi; \psi, \eta) = \frac{1}{2}[a(\eta, \psi) + a(\psi, \eta)]$$

In particular for all φ and ψ in V

$$(11) \quad J(\varphi) = J(\psi) + dJ(\psi; \varphi - \psi) + \frac{1}{2}d^2J(\psi; \varphi - \psi, \varphi - \psi).$$

In view of equation (1) for u

$$(12) J(v) = J(u) + \frac{1}{2}a(v-u, v-u), \quad \forall v \in V.$$

If u_h is the solution of (1_h),

$$(13) \|u_h - u\|_V^2 = a(u_h - u, u_h - u) = 2[J(u_h) - J(u)],$$

where we use $\sqrt{a(v, v)}$ as the norm on V . If τ_h and τ'_h are two triangulations of Ω with respective solutions $u_h \in V_h$ and $u'_h \in V_h$, then

$$\|u'_h - u\|_V^2 = \|u_h - u\|_V^2 + 2[J(u'_h) - J(u_h)].$$

So to decrease the error $\|u_h - u\|_V$ associated with τ_h , it suffices to find a new triangulation τ'_h , and hence new set of positions M' of the variable nodes, such that

$$(14) J(u'_h) < J(u_h).$$

In order to formalize the "optimal triangulation" problem, it is helpful to explicitly denote the dependence of the solution u_h to (1_h) on the triangulation τ_h

$$(15) u_h = u_h(\tau_h)$$

and the dependence of the triangulation τ_h on the set of variable nodes M by

$$(16) \tau_h = \tau_h(M).$$

In addition we introduce the notation

$$(17) j(M) = J(u_h(\tau_h(M)))$$

for the dependence of the optimal cost with respect to M . Recall that

$$(18) J(u_h) = \text{Inf}\{J(\varphi_h) : \varphi_h \in V_h\}$$

$$(19) dJ(u_h; \varphi_h) = 0, \quad \forall \varphi_h \in V_h.$$

Formally, the "optimal triangulation" problem would be to find the solution of the following minimisation problem:

$$(20) \text{ Inf}\{j(M) : M \subset (\mathbb{R}^n)^P, M \subset \bar{\Omega}\},$$

where $\bar{\Omega}$ is the closure of Ω .

A difficulty with the formulation (20) is the fact that some choices of positions might yield unacceptable triangulations $\tau_h(M)$. To get around this difficulty, we restrict our attention to a family \mathcal{M}_T of sets of variable nodes M which generate a triangulation with a common topological table T : for any two triangulations "corresponding nodes" will have "corresponding neighbouring nodes". To be more specific, fix the nodes at the vertices of the domain Ω and the number p of variable nodes. Define the family of sets of variable nodes which generate a triangulation with a given topological table T :

$$(21) \mathcal{M}_T = \{M \subset (\mathbb{R}^n)^P \mid M \subset \bar{\Omega} \text{ and } \tau_h(M) \in \tau_T\},$$

where τ_T is the family of all triangulations of $\bar{\Omega}$ with the same topological table T . In view of the above definition we can consider the new minimization problem:

$$(22) \text{ Inf } \{j(M) \mid M \in \mathcal{M}_T\}.$$

If a minimizing element \hat{M} exists, it will generate the "optimal triangulation" $\hat{\tau}_h = \tau_h(\hat{M})$ with respect to the family \mathcal{M}_T of sets of variable nodes M , which generate a triangulation $\tau_h(M)$ with the topological table T .

4. GRADIENT COMPUTATIONS

The object of this section is the computation of the partial derivatives of j

$$(25) \frac{\partial j}{\partial M_i^\ell}, \quad 1 \leq \ell \leq n, \quad 1 \leq i \leq p,$$

with respect to the coordinates of the position

$$(26) M_i = \{x_i^\ell | 1 \leq \ell \leq N\}$$

of each variable node M_i . The starting point is the cost function

$$(27) J(u_h) = -\frac{1}{2} \langle F, u_h \rangle = j(M) = -\frac{1}{2} \langle F, u_h(\tau_h(M)) \rangle,$$

where u_h is the solution of the variational equation (1_h). Although the partial derivatives of j can be computed by various techniques, we shall promote the use of partial Eulerian derivatives $\dot{u}_{x_i}^\ell$ as developed in the work of J.P.Zolésio [1,2].

4.1 Partial Eulerian Derivatives

We briefly recall the speed method for boundary value problems over smooth domains Ω . Given a smooth deformation field V defined in a neighbourhood of Ω , each point X in Ω at time $t=0$ is transported into a point $x(t)$ at time $t > 0$ through the differential equation

$$(28) \frac{dx}{dt}(t) = V(t, x(t)), \quad x(0) = X.$$

This induces a smooth transformation $T_t(V)X = x(t)$ which maps Ω onto $\Omega_t = T_t(V)(\Omega)$. The Eulerian derivative of the cost function J at Ω for the field V is defined as (cf. J.P.Zolésio [1,2])

$$(29) dJ(\Omega; V) = \left. \frac{d}{dt} J(\Omega_t) \right|_{t=0}.$$

In the discrete case, the state $u_h = u_h(\tau_h)$ (solution of equation (1_h)) depends on the variable nodes M through the triangulation $\tau_h = \tau_h(M)$. Denote by $\{l_\ell | 1 \leq \ell \leq n\}$ the basis of R^n , where l_ℓ is the n -tuple which has a 1 in the ℓ -th position and zeros everywhere else. Given a small $t > 0$ and a node M_i , we perturb the set of positions M in the ℓ -th direction

$$(30) M_{i\ell}^t = \{M_j + t\delta_{ij}l_\ell | 1 \leq j \leq p\}$$

where δ_{ij} is the Kronecker index function. In each case, we construct vector fields which will transport triangles of τ_h onto triangles of the new τ_h^t and shape functions

$$(31) b = \{b_j | 1 \leq j \leq p+q\} \subset V_h$$

for τ_h onto shape functions

$$(32) b^t = \{b_j^t | 1 \leq j \leq p+q\} \subset V_h^t$$

for τ_h^t :

$$(33) b_j(M_i) \quad (\text{resp. } b_j^t(M_i^t)) = \delta_{ij}, \quad 1 \leq i, j \leq p+q.$$

J.P. Zolésio [2] has shown that an appropriate choice is

$$(34) V_{i\ell}(t, x) = e_i(x)l_\ell, \quad 1 \leq \ell \leq n, \quad 1 \leq i \leq p,$$

where the set $e = \{e_i | 1 \leq i \leq p\}$ are the piecewise linear (P^1) shape functions: for all i , $1 \leq i \leq p$

$$(35) \begin{cases} e_i \in \{v \in H^1(\Omega_h) | v|_K \in P^1(K), \forall K \in \tau_h\} \\ e_i(M_j) = \delta_{ij}, \quad 1 \leq j \leq p+q. \end{cases}$$

The remarkable feature of the deformation field $V_{i\ell}$ is the fact that it maps each triangle of τ_h onto a triangle of τ_h^t and each basis element b_j onto the corresponding basis element b_j^t . Moreover, if u is a solution of the boundary value problem in V_h^t , then the transported solution

$$(36) u_{i\ell}^t = u_t \circ T_t(V_{i\ell})$$

belongs to V_h . Thus the partial material derivative of u with respect to the ℓ -th component of the position of node M_i is an element of V_h defined as

$$(37) \dot{u}_{i\ell} = \left. \frac{du_{i\ell}^t}{dt} \right|_{t=0}$$

and the partial Eulerian derivative of j as

$$(38) \frac{\partial j}{\partial M_i^{\ell}} = dj(M; V_{i\ell})$$

where

$$(39) j(M) = J(u_h(\tau_h(M))).$$

4.2 Application to the Dirichlet problem

Choose $V = H_0^1(\Omega)$

$$(40) a(u, v) = \sum_{i,j=1}^n \int_{\Omega_h} a_{ij} \frac{\partial u}{\partial x_j} \frac{\partial v}{\partial x_i} d\Omega + \int_{\Omega_h} a_0 uv d\Omega$$

where $a_0 \in L^\infty(\Omega)$, $a_{ij} \in L^\infty(\Omega)$ and for all x in Ω

$$(41) \begin{cases} a_0(x) \geq 0, a_{ij}(x) = a_{ji}(x), 1 \leq i, j \leq n, \\ \exists \alpha > 0, \sum_{i,j=1}^n a_{ij}(x) \xi_j \xi_i \geq \sum_{i=1}^n \xi_i^2, \forall \xi = \{\xi_i\}_{i=1}^n \end{cases}$$

$(L^\infty(\Omega))$ is the space of essentially bounded functions on Ω . F is of the form

$$(42) \langle F, v \rangle = \int_{\Omega} f v d\Omega,$$

for a function f in $L^2(\Omega)$. The solution of problem (1) with this choice of V , a and F coincides with the solution of the Dirichlet boundary value problem:

$$(43) \begin{cases} Au = f & \text{in } \Omega, \\ u = 0 & \text{on } \Gamma. \end{cases} \quad Au = - \sum_{i,j=1}^n \frac{\partial}{\partial x_i} (a_{ij} \frac{\partial u}{\partial x_j}) + a_0 u$$

(the boundary of Ω).

The solution of (1), (7) and (36) coincide. The solution of $(1)_h$ is the finite element approximation which coincides with the solution of the minimization problem $(7)_h$. Recall that from identity (27)

$$(44) j(M) = J(u_h(\tau_h(M))) = - \frac{1}{2} \int_{\Omega} f u_h d\Omega.$$

For small $t > 0$

$$(45) j(M+tV) = - \frac{1}{2} \int_{\Omega^t} f(u_h)_t d\Omega^t$$

where V stands for one of the deformation fields $V_{i\ell}$, $\Omega^t = T_t(\Omega)$,

and $(u_h)_t$ is the solution of the variational problem

$$(46) \sum_{i,j=1}^n \int_{\Omega^t} a_{ij} \frac{\partial (u_h)_t}{\partial x_j} \frac{\partial v_h}{\partial x_i} d\Omega^t = \int_{\Omega^t} f v_h d\Omega^t, \quad \forall v_h \in V_h^t$$

or in vectorial form

$$(46a) \int_{\Omega^t} (\underline{A} \nabla u_h, \nabla v_h) d\Omega^t = \int_{\Omega^t} f v_h d\Omega^t, \quad \forall v_h \in V_h^t$$

where ∇u_h and ∇v_h denote the gradients in R^n and \underline{A} is the symmetrical matrix whose entries are $\{a_{ij}\}$. By introducing the transported solution

$$(47) u_h^t = (u_h)_t \circ T_t(V),$$

identity (45) can be rewritten on Ω_h

$$(48) j(M+tV) = - \frac{1}{2} \int_{\Omega} J_t(f \circ T_t) u_h^t d\Omega,$$

where J_{T_t} is the determinant of the Jacobian $\overset{DT}{V}$ of the transformation $T_t(V)$. It is readily seen (cf. J.P.Zolésio [2]) that

$$(49) \quad dj(M;V) = -\frac{1}{2} \int_{\Omega} [\text{div}(fV(0))u_h + f\dot{u}] d\Omega$$

where $V(0)$ is the function $x \rightarrow V(0,x)$ and \dot{u} is the solution of the variational equation

$$(50) \quad \begin{cases} \dot{u} \in V_h, & \forall v \in V_h \\ \int_{\Omega} (\underline{A} \nabla \dot{u}, \nabla v) d\Omega = \int_{\Omega} [-(\underline{Q}' \nabla u_h, \nabla v) + \text{div}(fV(0))v] d\Omega \end{cases}$$

where

$$(51) \quad \underline{Q}' = \text{div}V(0)\underline{A} - [DV(0)\underline{A} + \underline{A}(DV(0))^*]$$

and $(DV(0))^*$ denotes the transpose of $DV(0)$. For $V = V_{i\ell}$ the $\alpha\beta$ element of the matrix \underline{Q}' is given by

$$(52) \quad \underline{Q}'_{\alpha\beta} = \partial_{\ell} e_i^{\alpha} \delta_{\alpha\beta} - \sum_{\gamma=1}^n [\partial_{\gamma} e_i^{\alpha} \delta_{\gamma\beta} \delta_{\alpha\ell} + \partial_{\alpha} e_i^{\alpha} \delta_{\alpha\gamma} \delta_{\beta\ell}]$$

where $\partial_m e_i$ denotes the partial derivative of $e_i(x)$ with respect to the component x_m . For instance for $n=2$ and $\underline{A}=\underline{I}$ (identity in \mathbb{R}^2)

$$(52a) \quad \underline{Q}' = \begin{bmatrix} -\partial_1 e_i & -\partial_2 e_i \\ -\partial_2 e_i & \partial_1 e_i \end{bmatrix} \quad \text{for } V = V_{i1}$$

$$(52b) \quad \underline{Q}' = \begin{bmatrix} \partial_2 e_i & -\partial_1 e_i \\ -\partial_1 e_i & -\partial_2 e_i \end{bmatrix} \quad \text{for } V = V_{i2}$$

Since \dot{u} belongs to V_h and u_h is the solution of the variational equation

$$(53) \quad \int_{\Omega} (\underline{A} \nabla u_h, \nabla v_h) d\Omega = \int_{\Omega} f v_h d\Omega, \quad \forall v_h \in V_h,$$

the above equation is true for $v_h = \dot{u}$. But the right-hand-side of (53)

with $v_h = \dot{u}$ is equal to the right-hand-side of (50) with $v = u_h$ since \underline{A} is symmetrical. Hence

$$(54) \int_{\Omega} f \dot{u}_h d\Omega = \int_{\Omega} [-(\mathcal{L}' \nabla u_h, \nabla u_h) + \text{div}(fV(0))u_h] d\Omega.$$

The substitution of the last identity in expression (49) for the gradient yields

$$(55) dj(M;V) = \frac{1}{2} \int_{\Omega} [(\mathcal{L}' \nabla u_h, \nabla u_h) - 2 \text{div}(fV(0))u_h] d\Omega.$$

THEOREM 1 (Dirichlet problem). The partial derivative of j with respect to the position of node $M_i = \{x_i^{\ell} | 1 \leq \ell \leq n\}$ are given by the following expression

$$(56) \frac{\partial j}{\partial x_i^{\ell}}(M) = \frac{1}{2} \int_{\Omega} \partial_{\ell} e_i \sum_{\alpha, \beta=1}^n a_{\alpha\beta} \partial_{\beta} u_h \partial_{\alpha} u_h d\Omega \\ - \frac{1}{2} \int_{\Omega} \sum_{\alpha, \gamma=1}^n [\partial_{\alpha} e_i a_{\alpha\gamma} + \partial_{\gamma} e_i a_{\gamma\alpha}] \partial_{\alpha} u_h \partial_{\gamma} u_h d\Omega \\ - \int_{\Omega} [\partial_{\ell} f e_i + f \partial_{\ell} e_i] u_h d\Omega. \quad \square$$

When $n=2$ and $\underline{A}=I$, expression (56) reduces to

$$(57a) \frac{\partial j}{\partial x_i^1}(M) = \int_{\Omega} \left\{ \frac{1}{2} \partial_1 e_i [(\partial_2 u_h)^2 - (\partial_1 u_h)^2] - \partial_2 e_i \partial_1 u_h \partial_2 u_h - \partial_1 (f e_i) u_h \right\} d\Omega$$

$$(57b) \frac{\partial j}{\partial x_i^2}(M) = \int_{\Omega} \left\{ \frac{1}{2} \partial_2 e_i [-(\partial_2 u_h)^2 + (\partial_1 u_h)^2] - \partial_1 e_i \partial_2 u_h \partial_1 u_h - \partial_2 (f e_i) u_h \right\} d\Omega.$$

It is readily seen that expression (56) is easily implementable since the terms $\partial_{\ell} e_i$ are non-zero only in a neighbourhood of the nodes M_i . The gradient can be constructed locally.

4.3 Application to the Neumann problem

Choose $V = H^1(\Omega)$, V_h the subspace of V

$$(58) V_h = \{v \in H^1(\Omega) \mid v|_K \in P^k(K), \forall K \in \tau_h\}$$

the bilinear form a as in (40) which verifies condition (41) and, in addition,

$$(59) a_0 \geq \alpha > 0.$$

Choose

$$(60) \langle F, v \rangle = \int_{\Omega} f v d\Omega + \int_{\Gamma} g v d\Gamma$$

where f is a function in $L^2(\Omega)$, Γ is the boundary of Ω , and g a function of $H^{-1/2}(\Gamma)$. If u is the solution of the variational equation

$$(61) a(u, v) = \langle F, v \rangle \quad \forall v \in V,$$

then u coincides with the solution of the Neumann boundary value problem

$$(62) \begin{cases} Au = f & \text{in } \Omega \quad (Au \text{ as defined in (43)}) \\ \frac{\partial u}{\partial n_A} = g & \text{on } \Gamma, \quad \frac{\partial u}{\partial n_A} = \sum_{i,j=1}^n a_{ij} \frac{\partial u}{\partial x_j} n_i \end{cases}$$

where $n = (n_1, \dots, n_n)$ is the unit exterior normal to the surface Γ .

We proceed as in section 4.2. The directional derivative of the functional

$$(63) j(M) = -\frac{1}{2} \left[\int_{\Omega} f u_h d\Omega + \int_{\Gamma} g u_h d\Gamma \right]$$

is given by

$$(64) dj(M; V) = -\frac{1}{2} \int_{\Omega} [\text{div}(fV(0)) u_h + f \dot{u}] d\Omega - \frac{1}{2} \int_{\Gamma} [\text{div}(gV(0)) u_h + g \dot{u}] d\Gamma,$$

since the boundary Γ of Ω is fixed. Free boundary nodes move along faces of Ω . The variational equation for the material derivative is

$$(65) \begin{cases} \dot{u} \in V_h, \quad \forall v \in V_h \\ \int_{\Omega} (\Delta \nabla \dot{u}, \nabla v) d\Omega = \int_{\Omega} [-(Q' \nabla u_h, \nabla v) + \text{div}(fV(0))] d\Omega + \int_{\Gamma} \text{div}(gV(0)) d\Gamma. \end{cases}$$

Since u_h is the solution of the variational equation

$$(66) \int_{\Omega} (\underline{A} \nabla u_h, \nabla v) d\Omega = \int_{\Omega} f v d\Omega + \int_{\Gamma} g v d\Gamma, \quad \forall v \in V_h,$$

it is verified with $v = \dot{u}$. Similarly (65) is verified with $v = u_h$. As a result

$$(67) \int_{\Gamma} g \dot{u} d\Gamma + \int_{\Omega} f \dot{u} d\Omega = \int_{\Omega} [-(\ell' \nabla u_h, \nabla u_h) + \text{div}(fV(0))] d\Omega + \int_{\Gamma} \text{div}(gV(0)) d\Gamma.$$

The substitution of the last identity into expression (64) yields

$$(68) dj(M; V) = \frac{1}{2} \int_{\Omega} [(\ell' \nabla u_h, \nabla u_h) - 2 \text{div}(fV(0)u_h)] d\Omega - \int_{\Gamma} \text{div}(gV(0)) d\Gamma.$$

But this is precisely expression (55) with an additional boundary term.

THEOREM 2. (Neumann problem). The partial derivatives of j with respect to the position of node $M_i = \{x_i^{\ell} | 1 \leq \ell \leq n\}$ are given by the following expression

$$(69) \frac{\partial j}{\partial x_i^{\ell}}(M) = \frac{1}{2} \int_{\Omega} \partial_{\ell} e_i \sum_{\alpha, \beta=1}^n a_{\alpha\beta} \partial_{\beta} u_h \partial_{\alpha} u_h d\Omega \\ - \frac{1}{2} \int_{\Omega} \sum_{\alpha, \gamma=1}^n [\partial_{\alpha} e_i a_{\alpha\gamma} + \partial_{\gamma} e_i a_{\gamma\alpha}] \partial_{\alpha} u_h \partial_{\gamma} u_h d\Omega \\ - \int_{\Omega} \partial_{\ell} (f e_i) u_h d\Omega - \int_{\Gamma} \partial_{\ell} (g e_i) u_h d\Gamma. \quad \square$$

4.4 Extension to Other Second Order Elliptic Problems

Any problem which can be abstracted in the form (1) can be handled by the techniques in the previous sections. Only slight modifications are to be brought to the final expression in Theorems 1 or 2. Certain families of non-symmetric elliptic problems can also be handled by appropriate choice of space dependent coefficients a_0 and a_{ij} .

4.5 Extension to higher even order elliptic problems

The reader will certainly have noticed that most of our analysis extends to fourth or higher even order elliptic problems. For a fourth order problem, V can be chosen as a closed subspace of the Sobolev space $H^2(\Omega)$ and V_h can again be given by expression (3). However this results in a different type of finite element approximation.

For second order problems

$$V_h \subset V \subset H^1(\Omega)$$

and the elements of V_h are continuous on $\bar{\Omega}$ (i.e. C^0 -approximation). For fourth order problems

$$V_h \subset V \subset H^2(\Omega)$$

and the elements of V_h are continuous in $\bar{\Omega}$ with continuous first order partial derivatives on $\bar{\Omega}$ (i.e. C^1 -approximation). In the computation of the partial Eulerian derivatives we have constructed a velocity vector field $V_{i\ell}(t,x)$ which transports triangles onto triangles and shape functions onto shape functions. For C^1 -approximations shape functions are distorted and are not transported onto shape functions. Thus higher even order problems require a deeper analysis which will eventually yield additional terms in the gradient expressions. However this is beyond the scope of the present paper.

5. Control parameters

When the number of variable nodes is large, it is customary to introduce a reduced set of control parameters $\ell = \{\ell_k | 1 \leq k \leq m\}$ to control the position of the set of nodes. This construction which depends on physical and computational considerations can be written

$$(70) \quad M = M(\ell),$$

and the cost function becomes a function L of ℓ

$$(71) \quad L(\ell) = j(M(\ell)) = J(u_h(\tau_h(M(\ell)))).$$

As a result using the chain rule,

$$(72) \quad \frac{\partial L}{\partial \ell_k} = \sum_{\alpha=1}^n \sum_{i=1}^p \frac{\partial j}{\partial x_i^\alpha} \frac{\partial x_i^\alpha}{\partial \ell_k}$$

where

$$(73) \quad M_i = \{x_i^\alpha | 1 \leq \alpha \leq n\}.$$

are the coordinates of node M_i .

An example of such a parametrization will be given in section 6.2.

6. Numerical Tests.

We have chosen two very simple numerical tests in order to illustrate the applications of the previous theory : a one-dimensional and a two-dimensional example.

6.1 One-dimensional example

Consider the Dirichlet boundary value problem

$$(74) \quad \begin{cases} -\frac{d^2 u}{dx^2} = f(x) & \text{in } \Omega =]0,1[\\ u(0) = u(1) = 0. \end{cases}$$

Partition the interval $[0,1]$ into N intervals

$$(75) \quad 0 = M_1 < M_2 < \dots < M_N < M_{N+1} = 1, \quad h_i = M_{i+1} - M_i, \quad 1 \leq i \leq N.$$

The approximation u_h of u is obtained by minimizing the functional

$$(76) \quad J(u_h) = \int_0^1 \left\{ \left(\frac{du_h}{dx} \right)^2 - f(u_h) \right\} dx$$

over the subspace

$$(77) \quad V_h = \left\{ v_h \mid v_h \in C^0(0,1), \quad v_h \text{ linear on each } [M_i, M_{i+1}], \right. \\ \left. v_h(0) = v_h(1) = 0 \right\}.$$

The set of nodes \bar{M} is given by :

$$(78) \quad \bar{M} = \{M_n \mid 1 \leq n \leq N+1\}, \quad \partial M = \{M_1, M_{N+1}\} \\ M = \{M_n \mid 2 \leq n \leq N\}.$$

Example 1. $\Omega = [0,1]$.

$$(79) \quad f = -2a, \quad a > 0 \text{ a constant.}$$

The solution to (74) is given by :

$$(80) \quad u(x) = a x(x-1)$$

The starting point is an unbalanced discretization concentrated on the left

$$(81) \quad M_n = \frac{(n-1)}{100}, \quad 0 \leq n \leq 10, \quad M_n = 1, \quad N=11.$$

After 100 iterations the algorithm converges towards a uniform discretization

$$(82) \quad M_n = \frac{n-1}{10}, \quad 0 \leq n \leq 11.$$

Figures 1 to 10 show the solution and the position of the discretization nodes as the number of iterations increases.

Figures 11 and 12 give the cost and norm of the gradient as a function of the number of iterations.

Figures 13 and 14 give the positions of nodes 6 and 2 as a function of the number of iterations.

This example shows that the optimal discretization is regular. It would have been difficult to predict this result since the solution is a parabola symmetrical about the point $x = \frac{1}{2}$ for which a concentration of nodes would have been expected around $x = \frac{1}{2}$.

Example 2. $\Omega =]0, 1[$.

$$(83) \quad f(x) = -12a x(x-1), \quad a > 0.$$

The solution is given by

$$(84) \quad u(x) = a x(x^3 - 2x^2 + 1).$$

The starting point here is a uniform discretization

$$(85) \quad M_n = \frac{n-1}{10}, \quad 0 \leq n \leq 11, \quad N=11.$$

The algorithm converges in 13 iterations to a discretization concentrated in the center at point $x = \frac{1}{2}$.

Figures 15 to 20 show the solution and the position of the discretization nodes as the number of iterations increases.

Figures 21 and 22 give the cost and the norm of the gradient as a function of the number of iterations. Figures 23 and 24 give the positions of nodes 6 and 2 as a function of the number of iterations.

This example seems to support the conjecture that the non-uniformity of the discretization is a function of the variation in magnitude of the function f . Here f is a positive parabola centered at $x=\frac{1}{2}$ and the optimal discretization is concentrated around $x=\frac{1}{2}$.

Example 3. $\Omega =]0,1[$ and f is as in example 2.

The starting point is the non-uniform discretization

$$M_n = \frac{n-1}{100}, \quad 0 \leq n \leq 10, \quad M_n = 1, \quad N=11.$$

After 120 iterations the algorithm converges towards discretization concentrated at $x=\frac{1}{2}$ which was obtained in Example 2. Figures 25 and 26 give the cost and the norm of the gradient as a function of the number of iterations. Figure 27 and 28 give the positions of nodes 6 and 2 as the number of iterations increases.

In all three examples a gradient technique has been used. At step p , denoted by

$$M_i^p = \{M_i^p \mid 1 \leq i \leq N\}$$

the variables nodes. The new set

$$M^{p+1} = \{M_i^{p+1} \mid 1 \leq i \leq N\}$$

is given by

$$M_i^{p+1} = M_i^p - t g_i^p, \quad g_i^p = \text{gradient at step } p,$$

and a $t > 0$ must be determined in such a way that

$$j(M^{p+1})$$

is minimized with respect to t . A bounded interval for t can be obtained by writing

$$M_{i+1}^{p+1} - M_i^{p+1} = h_i^{p+1} > 0, \quad \forall i$$

which is equivalent to

$$0 < t < \frac{M_{i+1}^p - M_i^p}{|g_{i+1}^p - g_i^p|}, \quad \forall i=1,2,\dots,N$$

with $g_1 = g_N = 0$. As the result

$$(86) \quad t \in]0, t_{\max}[, \quad t_{\max} = \min_{1 \leq i \leq N} \frac{M_{i+1} - M_i}{|g_{i+1}^p - g_i^p|}.$$

6.2 Two-dimensional example

We have chosen a very simple example to illustrate the previous theoretical considerations. Given the domain

$$(87) \quad \Omega = \{(x_1, x_2) \mid |x_1 + x_2| < 1\} \subset \mathbb{R}^2$$

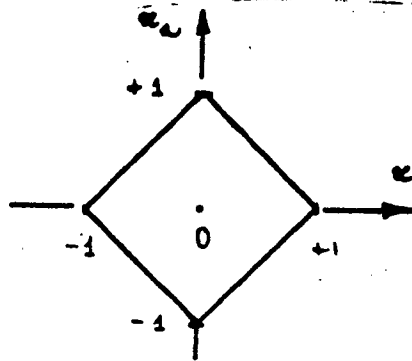


Figure 29 : Domain Ω .

Let u be the solution of the Dirichlet problem

$$(88) \quad \begin{cases} \frac{\partial^2 u}{\partial x_1^2} + \frac{\partial^2 u}{\partial x_2^2} + f = 0 & \text{in } \Omega \\ u = 0 & \text{on } \Gamma \text{ (boundary of } \Omega \text{)}. \end{cases}$$

This is equivalent to problem (1) with $V = H_0^1(\Omega)$,

$$(89) \quad a(u, v) = \int_{\Omega} [\partial_1 u \partial_1 v + \partial_2 u \partial_2 v] \, d\Omega$$

$$(90) \quad \langle F, v \rangle = \int_{\Omega} f v \, d\Omega$$

$$(91) \quad f(x_1, x_2) = (N+1)(N+2)(1 - |x_1| - |x_2|)^N$$

for $N = 6$.

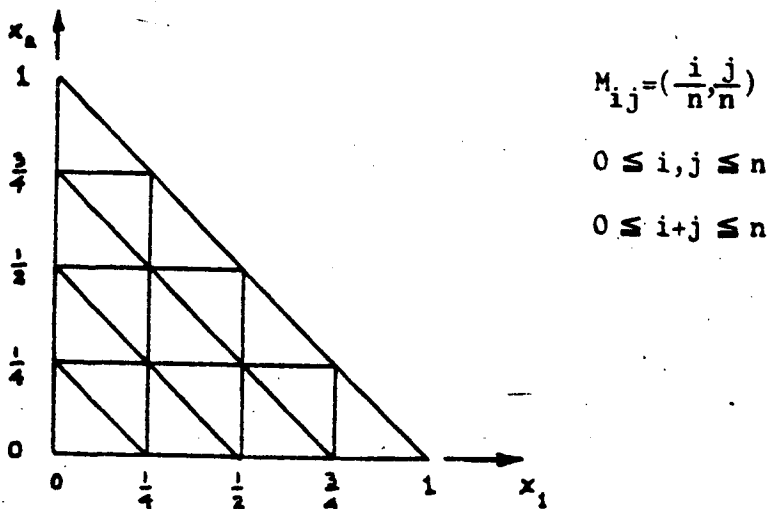


Figure 30 : Initial triangulation T_h for $n=4$.

Since the problem is symmetrical with respect to the x_1 and x_2 axes, it is convenient to only triangularize the first quadrant (cf. Fig. 30).

The sets of nodes are :

$$(92) \quad \bar{M} = \{M_{ij} \mid 0 \leq i, j \leq n, 0 \leq i+j \leq n\}, \quad M_{ij} = \left(\frac{i}{n}, \frac{j}{n}\right)$$

$$(93) \quad \partial M = \{M_{on}, M_{no}\}, \quad M = \{M_{ij} \in \bar{M} \mid M_{ij} \in \partial M\}.$$

Two types of experiments were run on this example. In the first one all the nodes in the triangulation were left free except boundary nodes which were required to stay on the boundary.

In the second experiment, the interior nodes were controlled by a parameter $\lambda \geq 1$.

6.2.1 Free interior nodes

Successive triangulations are shown in Figures 31 to 41. The experiment was stopped at iteration 12 (Figure 41) since three triangles collapsed. At the next iteration one or two nodes can go across the side of a triangle. This creates artificial or overlapping triangles which destroy the initial topology of the triangulation.

There are many ways to avoid or control this phenomenon. The simplest one is to introduce control parameters which will always preserve the topology of the initial triangulation. This technique will be successfully used in section 6.2.3.

In this section it is fair to say that the algorithm behaved nicely up to iteration 12.

As in the one-dimensional example of section 6.1 a constraint was placed on the scalar parameter t

$$(94) \quad 0 < t < t_{\max}$$

to preserve the initial triangulation.

Given a triangle T defined by the coordinates of its vertices

$$M_1 = (x_{11}, x_{12}) \quad M_2 = (x_{21}, x_{22}) \quad M_3 = (x_{31}, x_{32})$$

and the corresponding gradients at each vertex

$$g_1 = (g_{11}, g_{12}) \quad g_2 = (g_{21}, g_{22}) \quad g_3 = (g_{31}, g_{32})$$

we determine for a number $t > 0$ a new triangle with vertices

$$M_1^t = M_1 - t g_1, \quad M_2^t = M_2 - t g_2, \quad M_3^t = M_3 - t g_3.$$

We want to find a $t > 0$ such that the oriented surface of triangle $M_1^t M_2^t M_3^t$ be of the same sign as the oriented surface of triangle $M_1 M_2 M_3$.

Recall that the oriented surface of a triangle T defined by its vertices $M_1 M_2 M_3$ can be defined as the exterior product

$$(95) \quad \frac{1}{2}(M_3 - M_1) \times (M_2 - M_1).$$

This is a vector. However we are only interested in the algebraic quantity

$$(96) \quad A(M_3 - M_1, M_2 - M_1)$$

where $A: \mathbb{R}^2 \times \mathbb{R}^2 \rightarrow \mathbb{R}$ is defined as

$$(97) \quad A(v^1, v^2), (w^1, w^2) = \frac{1}{2}[v_1 w_2 - v_2 w_1]$$

Given a triangle T defined by its vertices $x_1 x_2 x_3$, compute its surface

$$A(M_3 - M_1, M_2 - M_1).$$

The parameter $t > 0$ defining a new triangle T^t from its vertices $M_1^t M_2^t M_3^t$ must be chosen in such a way that the surface of T^t be of the same sign as the surface of T

$$(98) \quad \text{sign } A(M_3^t - M_1^t, M_2^t - M_1^t) = \text{sign } A(M_3 - M_1, M_2 - M_1).$$

This yields a quadratic inequality in the variable t

$$(99) \quad a t^2 + b t + c \geq 0, \quad t \geq 0$$

where

$$(100) \quad \begin{aligned} a &= A(g_3 - g_1, g_2 - g_1) \text{sgn } A(M_3 - M_1, M_2 - M_1) \\ b &= -[A(M_3 - M_1, g_2 - g_1) + A(g_3 - g_1, M_2 - M_1)] \text{sgn } A(M_3 - M_1, M_2 - M_1) \\ c &= |A(M_3 - M_1, M_2 - M_1)| \geq 0 \end{aligned}$$

As a result $t=0$ is always an admissible (but useless) solution.

For each triangle T a range $[0, t_T]$ is determined. The bound t_{\max} is chosen as follows:

$$(101) \quad t_{\max} = \min \{t_T : T \in \mathcal{F}\}$$

and the parameter t must be chosen in the range

$$(102) \quad t \in [0, t_{\max}].$$

The computation of t_T for each triangle is not difficult since the coefficient c is always non negative :

$$a < 0 \Rightarrow b^2 - 4ac > 0 \Rightarrow t_T = \frac{-b - \sqrt{b^2 - 4ac}}{2a}$$

$$a \geq 0 \text{ i) } b^2 - 4ac \leq 0 \Rightarrow t_T = +\infty$$

$$\text{ii) } b^2 - 4ac > 0 \Rightarrow \frac{-b + \sqrt{b^2 - 4ac}}{2a} \leq t_T \\ \Rightarrow t_T = +\infty \text{ (} a \geq 0, c \geq 0 \text{)}$$

So the computations are extremely simple. There is a bound on t_T only in the case $a < 0$

$$(103) \quad t_T = \begin{cases} \frac{-b - \sqrt{b^2 - 4ac}}{2a} & , \text{ if } a < 0 \\ +\infty & , \text{ if } a \geq 0 \end{cases}$$

Obviously this technique has its numerical limitations as seen at iteration 12 (Figure 41) where errors in the computation of the coefficients a, b, c and/or the root can lead to a t which is too large. As some triangles shrink to zero surface this is likely to occur. When it does, it would be advisable to fix the triangulation around delinquent nodes and in the vicinity of collapsing triangles.

6.2.2 A gradient technique with thresholds

The fundamental difficulty in the method described in the previous section is that the ill-behaviour of a single triangle can reduce the size of the global t_{\max} to zero and essentially stop the whole optimization process.

Intuitively it would be desirable to set the gradient artificially to zero at nodes M_i belonging to ill-behaved triangles and let the other nodes move. To do this we use the construction of section 6.2.1 with some modifications.

Consider the variable node M_i and the set \mathcal{T}_i of all triangles T having x_i as a vertex.

$$(104) \quad \mathcal{T}_i = \{T \in \mathcal{T} \mid M_i \text{ is a vertex of } T\}.$$

For each T of \mathcal{F}_i compute the corresponding t_T .

Associate with each variable node M_i the parameter

$$(105) \quad t_i = \text{Min}\{t_T : T \in \mathcal{F}_i\}.$$

First method. Associate with each node M_i , the modified gradient

$$(106) \quad \bar{g}_i = \begin{cases} g_i & , \text{ if } t_i \geq \theta \\ 0 & , \text{ if } t_i < \theta \end{cases}$$

for some preset threshold $\theta > 0$. Once this computation has been done for each node M_i , the parameter t_{\max} is defined as

$$(107) \quad t_{\max}^{\theta} = \min\{\max[t_i, \theta] : M_i \in M\}.$$

We go back to our global optimization by moving each node M_i to a new position M_i^t

$$(108) \quad M_i^t = M_i - t \bar{g}_i$$

for some t , $0 < t \leq t_{\max}^{\theta}$. \square

Second method. Associate with each node M_i , the modified gradient

$$(109) \quad \bar{g}_i = \begin{cases} t_i g_i & , \text{ if } t_i \geq \theta \\ 0 & , \text{ if } t_i < \theta \end{cases}$$

for some preset threshold $\theta > 0$. Then we go back to our global optimization and move each node M_i^t to a new position M_i^t

$$(110) \quad M^t = M_i - t \bar{g}_i$$

for some t , $0 < t \leq 1$. \square

Both methods can be initiated with a large threshold θ which can be further decreased as needed or when nodes are not moving any more.

6.2.3 Nodes controlled by a parameter

We introduce a control parameter $\ell \geq 1$. The vertices of the (quarter of the) domain are

$$(111) \quad \partial M = \{(0,1), (1,0), (0,0)\}$$

and for an even integer $n \geq 2$

$$(112) \quad M = M_0 \cup M_1 \cup M_2 \cup M_3$$

where

$$(113) \quad M_0 = \{M_{ij}(\ell) \mid M_{ij}(\ell) = \left(\left(\frac{i}{n}\right)^\ell, \left(\frac{j}{n}\right)^\ell\right), 0 \leq i, j \leq n, 0 < i+j < n\}$$

$$(114) \quad M_1 = \{M_{ij}(\ell) \mid M_{ij}(\ell) = \left(\left(\frac{i}{n}\right)^\ell, 1 - \left(\frac{i}{n}\right)^\ell\right), \frac{n}{2} < i < n, i+j=n\}$$

$$(115) \quad M_2 = \{M_{\frac{n}{2}, \frac{n}{2}} = \left(\frac{1}{2}, \frac{1}{2}\right)\}$$

$$(116) \quad M_3 = \{M_{ij}(\ell) \mid M_{ij}(\ell) = \left(1 - \left(\frac{j}{n}\right)^\ell, \left(\frac{j}{n}\right)^\ell\right), \frac{n}{2} < j < n, i+j=n\}$$

The object of this exercise is to determine (for $N=6$ in expression (91)), the best ℓ in \mathbb{R} and hence the best triangulation within this family of triangulations. Intuitively as N increases a singularity is created around the center of the domain Ω which should result in a finer triangulation around the point $(0,0)$.

The derivative of the position of node M_{ij} in M_0 with respect to ℓ is

$$(113) \quad \frac{\partial M_{ij}}{\partial \ell}(\ell) = \left(\left(\frac{i}{n}\right)^\ell \ln\left(\frac{i}{n}\right), \left(\frac{j}{n}\right)^\ell \ln\left(\frac{j}{n}\right)\right).$$

For nodes in M_1 and M_3

$$(114) \quad \frac{\partial M_{i, n-i}}{\partial \ell} = \left(\frac{i}{n}\right)^\ell \ln\left(\frac{i}{n}\right) (1, -1), \quad \frac{n}{2} < i < n$$

$$(115) \quad \frac{\partial M_{n-j, j}}{\partial \ell} = \left(\frac{j}{n}\right)^\ell \ln\left(\frac{j}{n}\right) (-1, 1), \quad \frac{n}{2} < j < n.$$

The numerical tests are shown in Figures 42 to 45.

REFERENCES

- W.D.Bardfield [1], An optimal mesh generator for Lagrangian hydrodynamic calculations in two space dimensions, *J.Comput.Phys.* 6 (1970), 417-429.
- J. Céa [1], Optimization, theory and algorithm, Tata Institute, Springer-Verlag, 1978.
- Ph.G.Ciarlet [1], The finite element method for elliptic problems, North-Holland Publishing Company, Amsterdam, New York, 1978.
- G.M.McNeice and P.V.Marcial [1], Optimization of finite element grids based on minimum potential energy. Tech.Rep.No.7, Div. of Engineering, Brown University, Dept. of the Navy, Office of Naval Research, June 1971.
- R.J.Melosh and P.V.Marcial [1], An energy basis for mesh refinement of structural continua, *Int.J.Num.Meth.Engng.* 11 (1977), 1083-1091.
- Y. Seguchi, Y.Tomita and S.Hashimoto [1], Optimal finite element discretization based on two-factor decision criterion of potential energy and condition number, *Trans.Jap.Soc.Mech.Engrs.* 378.
- M.S.Shephard and R.H.Gallagher [1], Finite element grid optimization, American Society of Mechanical Engineers, 1979.
- M.S. Shephard, R.H.Gallagher and J.F.Abel [1], The synthesis of near-optimum finite element meshes with interactive computer graphics. *Int.J.Num.Meth.Engng* 15 (1980), 1021-1029.
- W.C.Tucker [1], A brief review of technique for generating irregular computational grids, *Int.J.Num.Meth.Engng* 15 (1980) 1335-1341.

J.P.Zolésio [1], The material derivative (or speed) method for shape optimization, in "Optimization of distributed parameter structures" Vol.II, pp.1089-1151, E.J.Haug and J.Céa, eds., Sijthoff and Noordhoff, Alphen aan den Rijn, The Netherlands, 1981.

[2], Les dérivées par rapport aux noeuds des triangulations et leur utilisation en identification de domaine, Ann.Sc.Mat. Québec 8 (1984), 97-120.

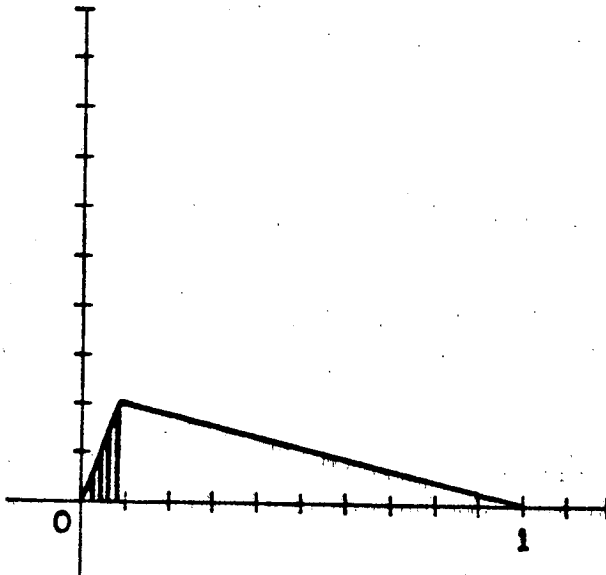


Figure 1. Example 1 : Initial discretization.

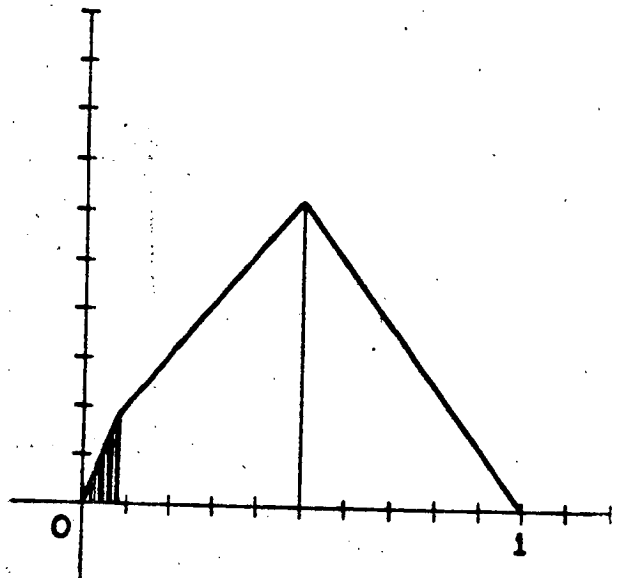


Figure 2. Example 1 : Second discretization.

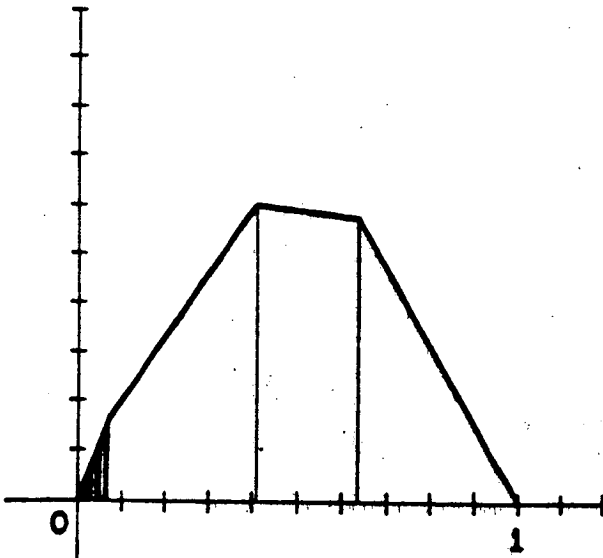


Figure 3. Example 1 ; Third discretization.

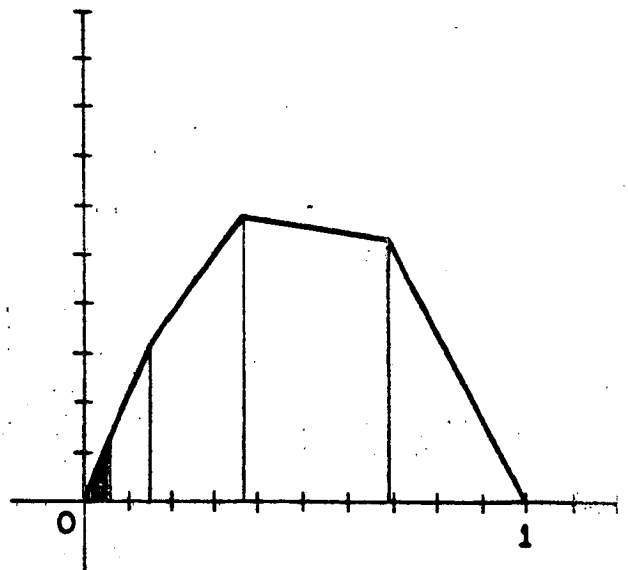


Figure 4. Example 1 : Fourth discretization.

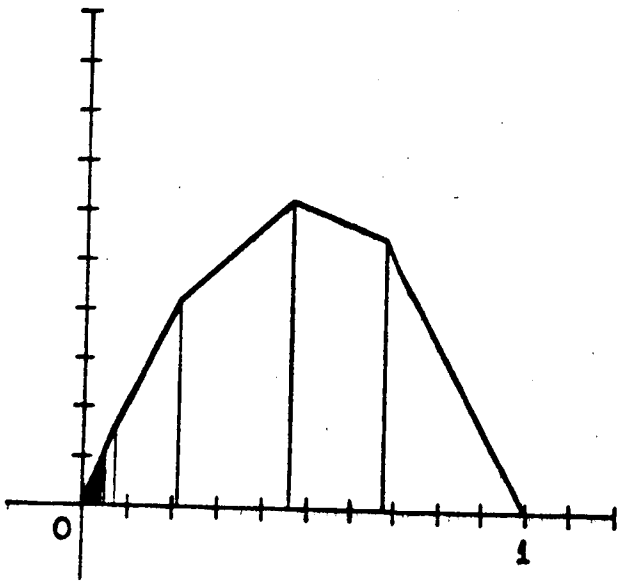


Figure 5. Example 1 : Fifth discretization.

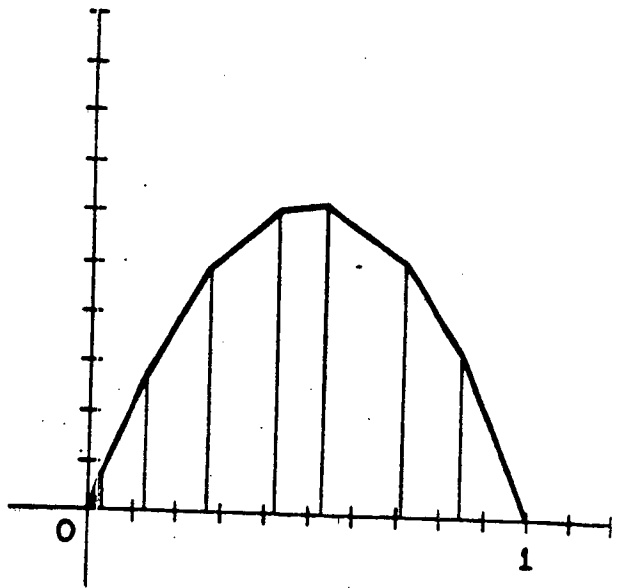


Figure 6. Example 1 : Tenth discretization.

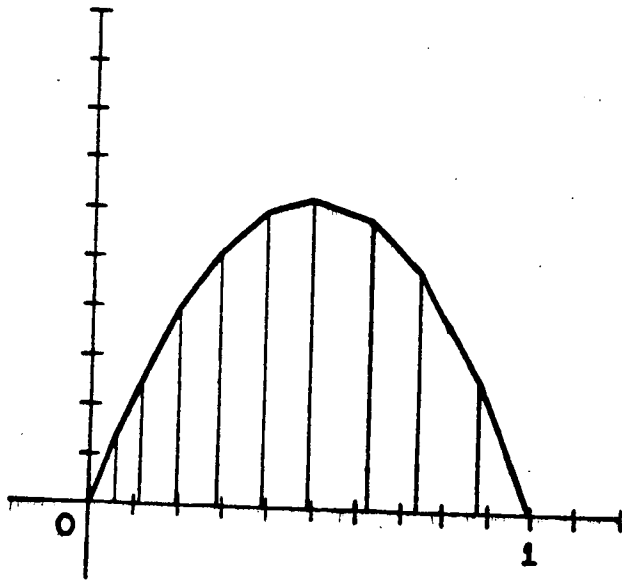


Figure 7. Example 1 : Twentieth discretization.

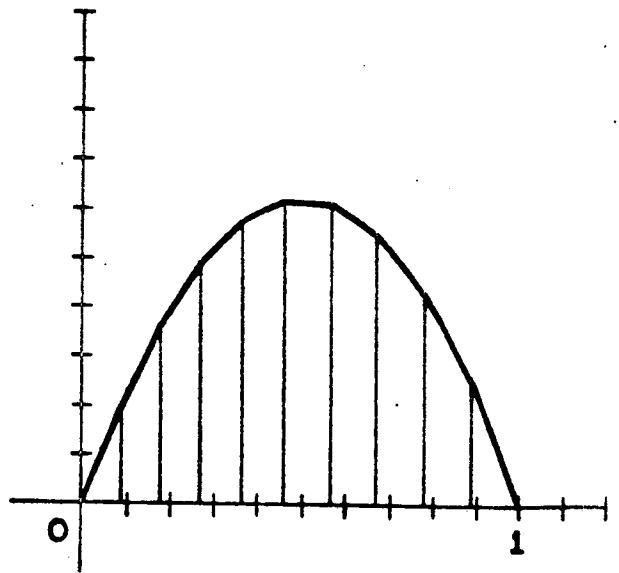


Figure 8. Example 1 : Fortieth discretization.

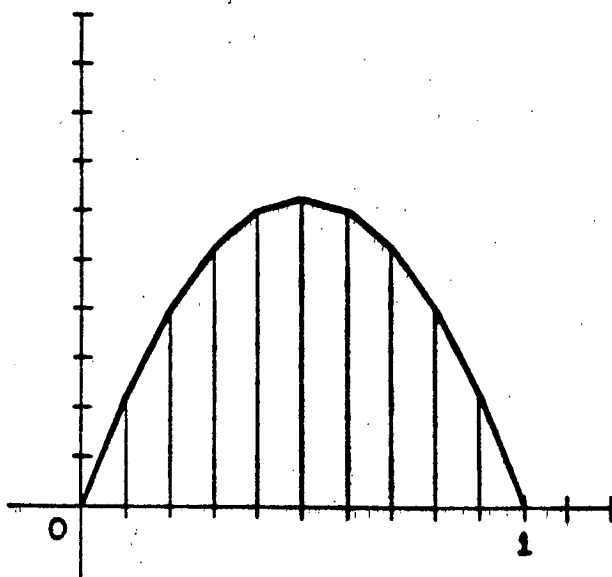


Figure 9. Example 1 : Sixtieth discretization.

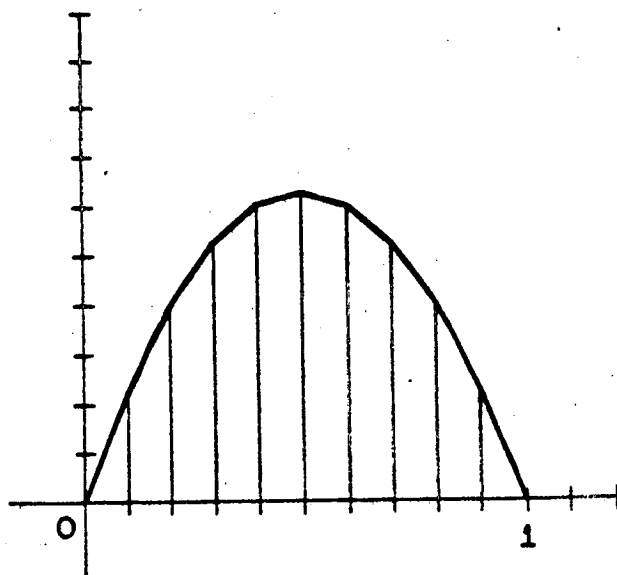


Figure 10. Example 1 : Final discretization.

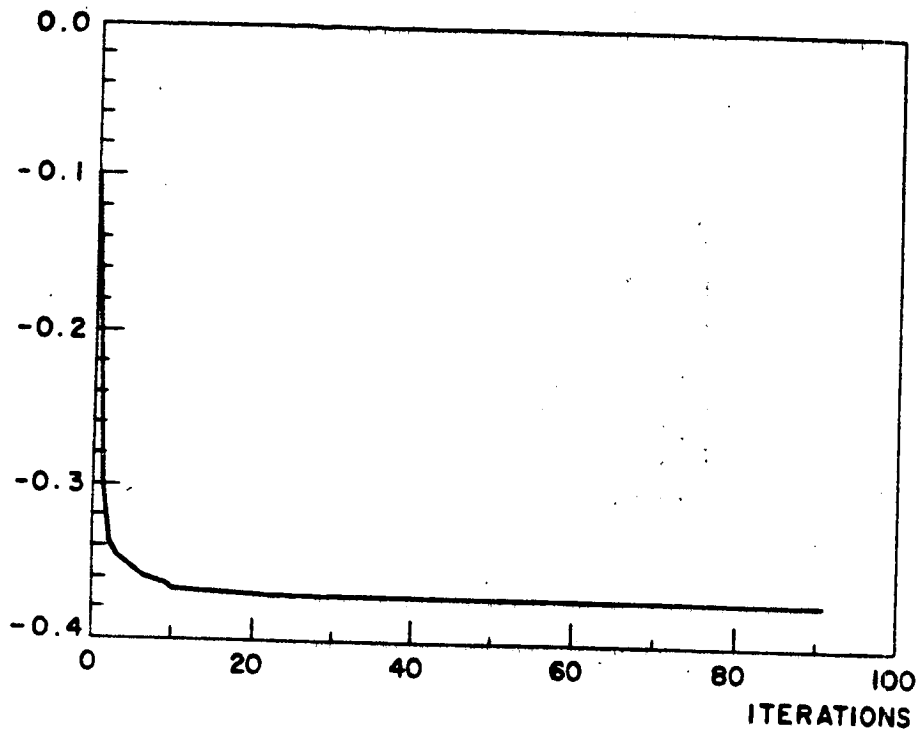


Figure 11. Example 1 : Variation of the cost as a function of the number of iterations.

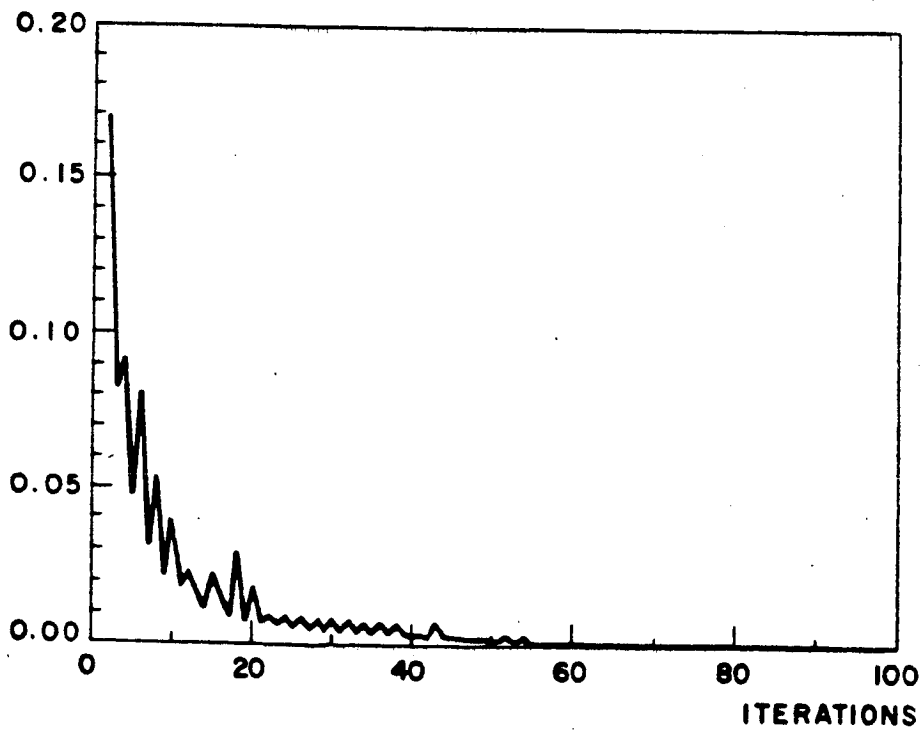


Figure 12. Example 1: Variation of the norm of the gradient as a function of the number of iterations.

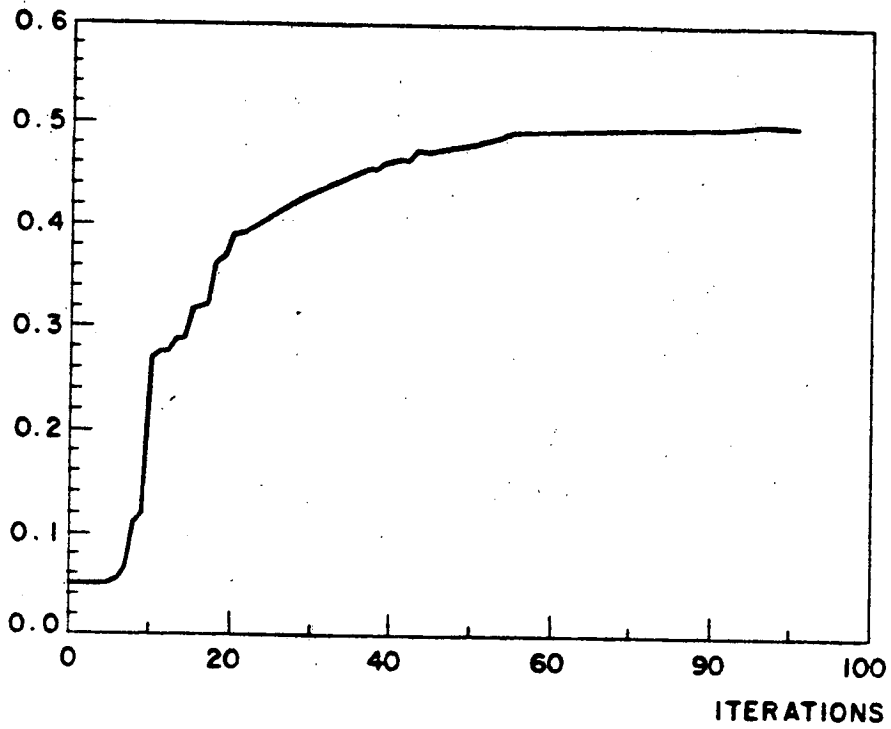


Figure 13. Example 1: Variation of the position of the sixth node as a function of the number of iterations.

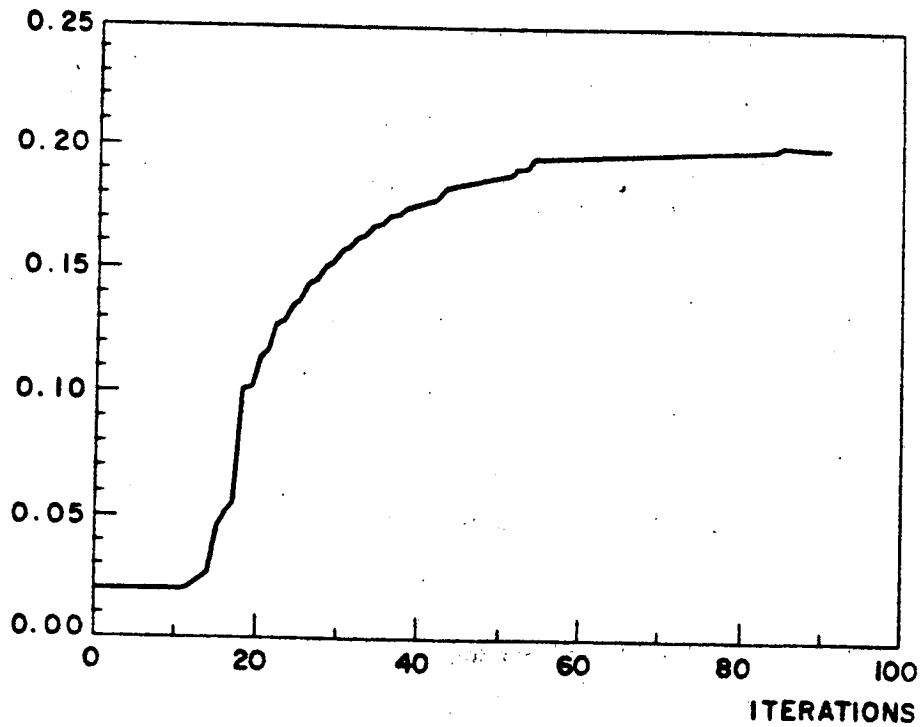


Figure 14. Example 1: Variation of the position of the second node as a function of the number of iterations.

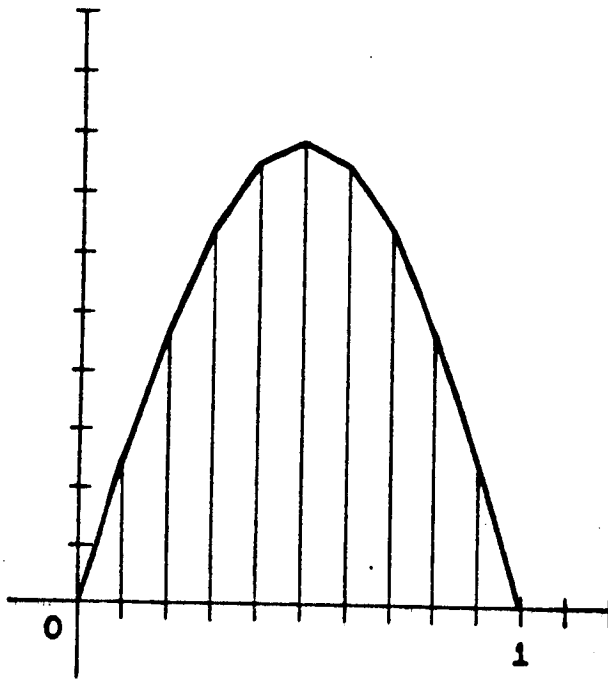


Figure 15: Example 2. Initial discretization.

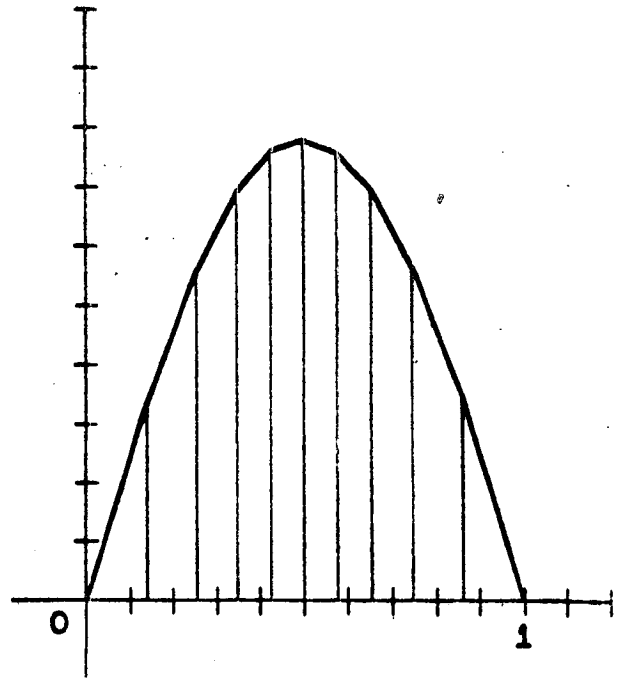


Figure 16: Example 2. Second discretization.

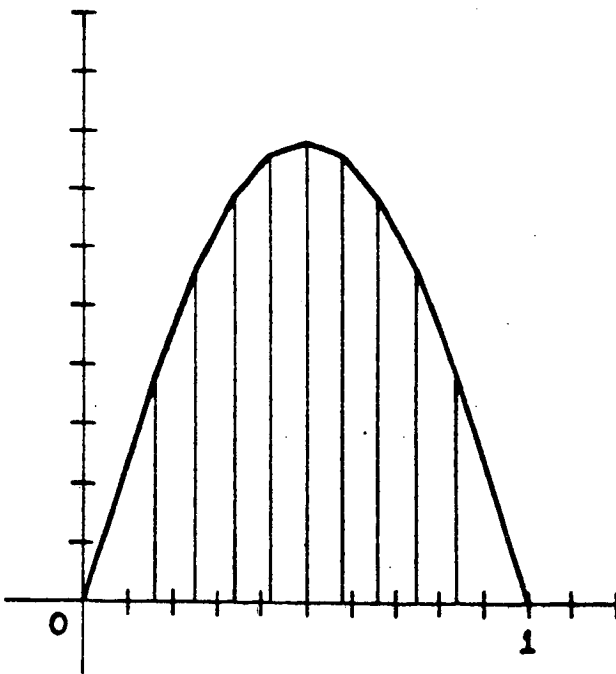


Figure 17: Example 2. Third discretization.

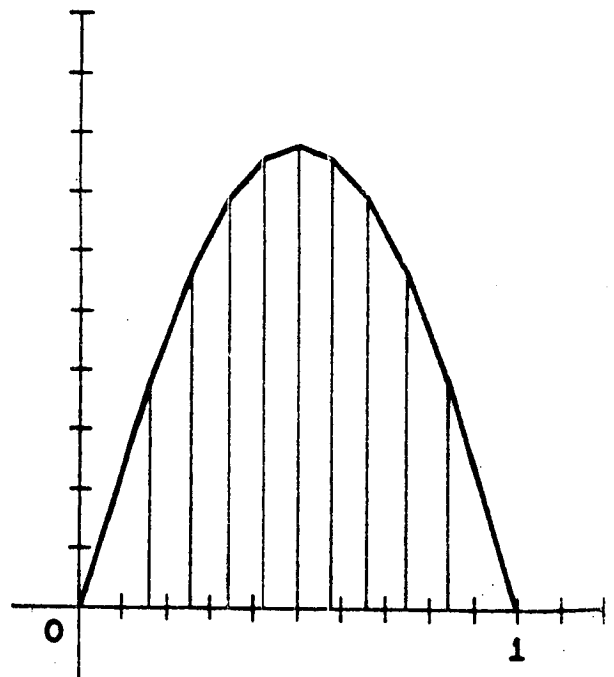


Figure 18: Example 2: Fifth discretization.

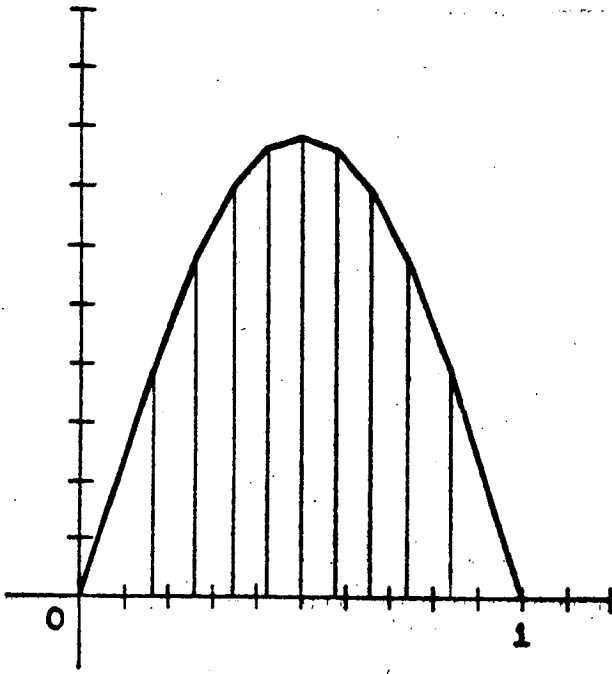


Figure 19. Example 2: Tenth discretization.

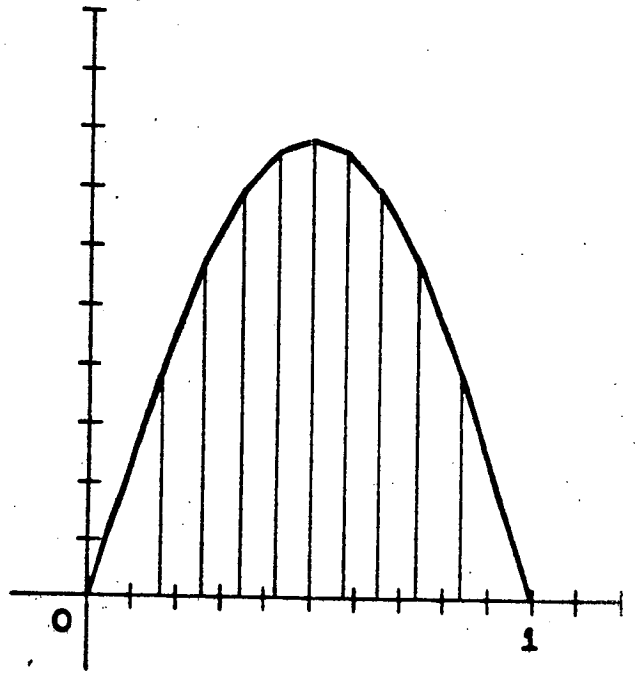


Figure 20. Example 2: last discretization.

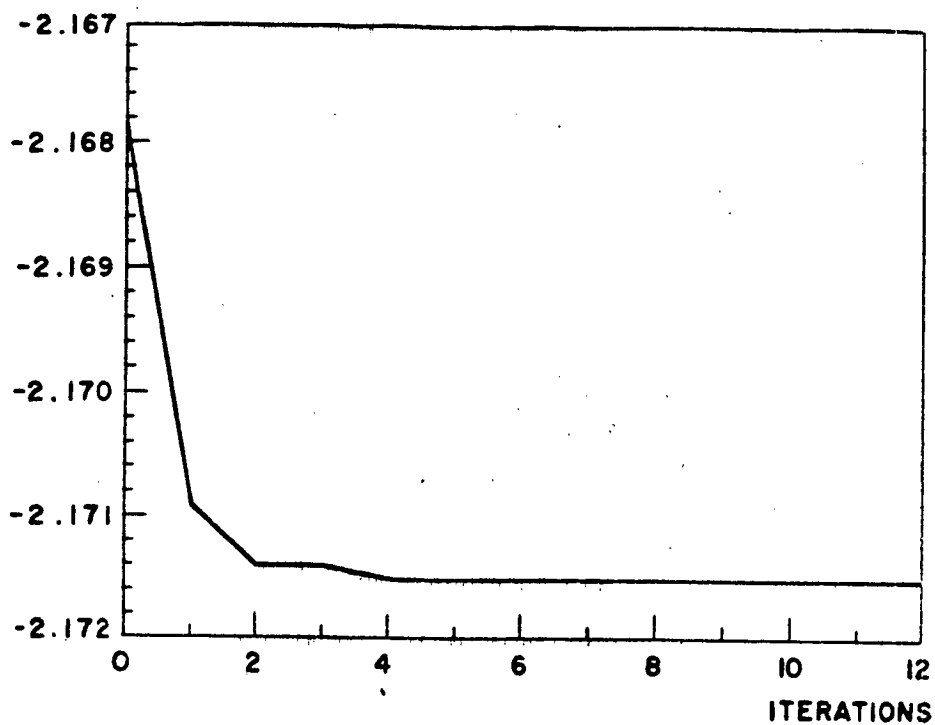


Figure 21. Example 2: Variation of the cost as a function of the number of iterations.

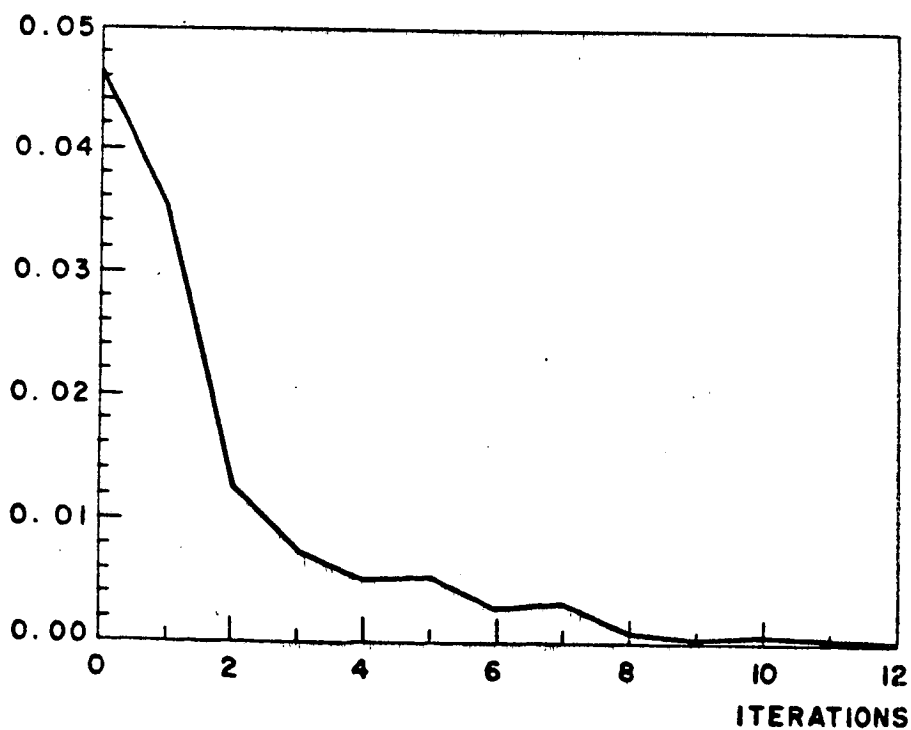


Figure 22. Example 2: Variation of the norm of the gradient as a function of the number of iterations.

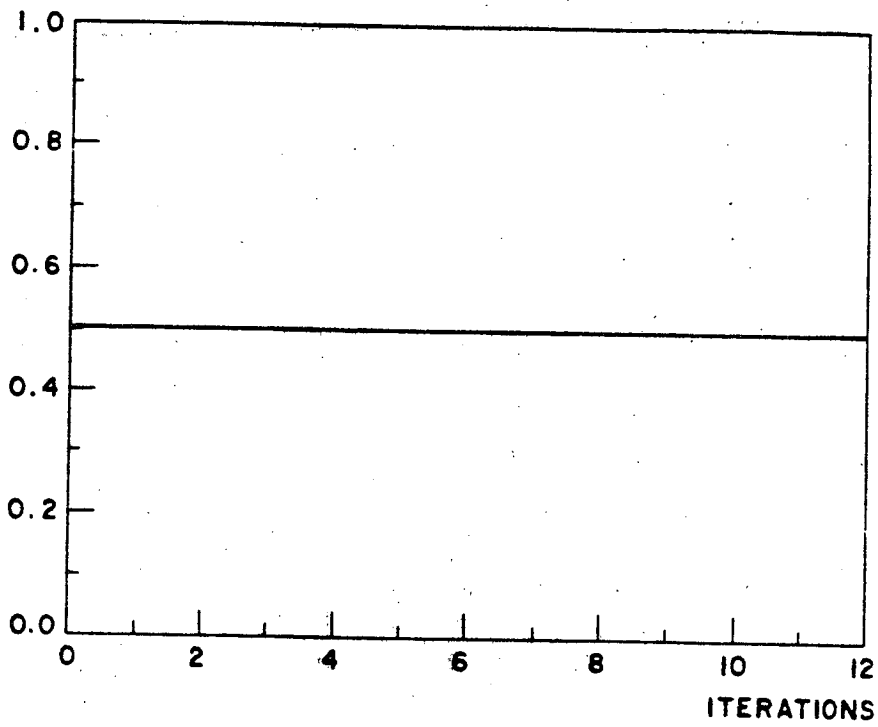


Figure 23. Example 2: Variation in the position of the sixth node as a function of the number of iterations.

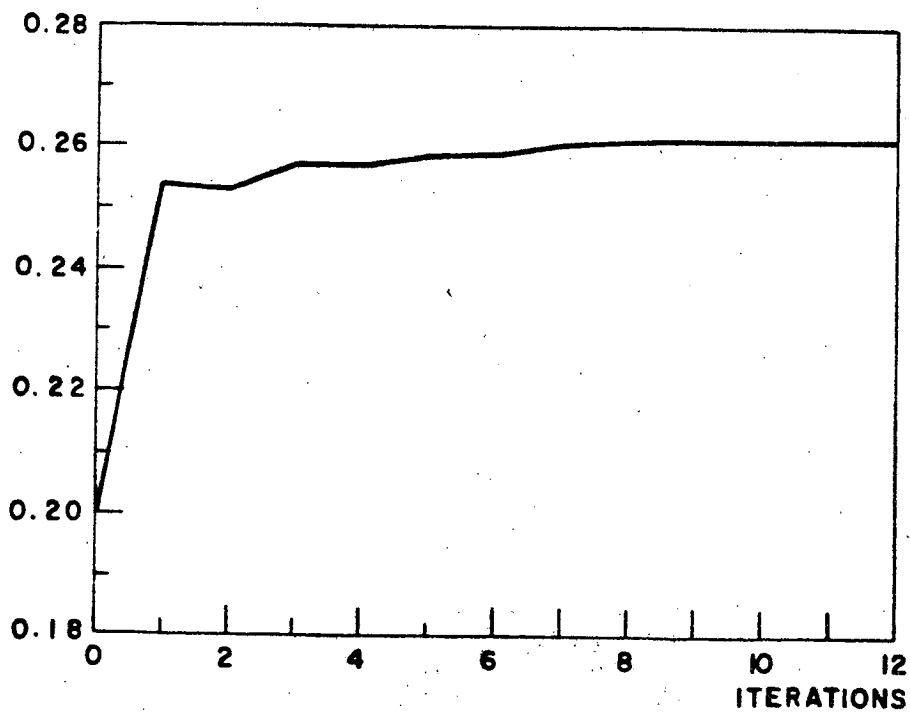


Figure 24. Example 2: Variation in the position of the second node as a function of the number of iterations.

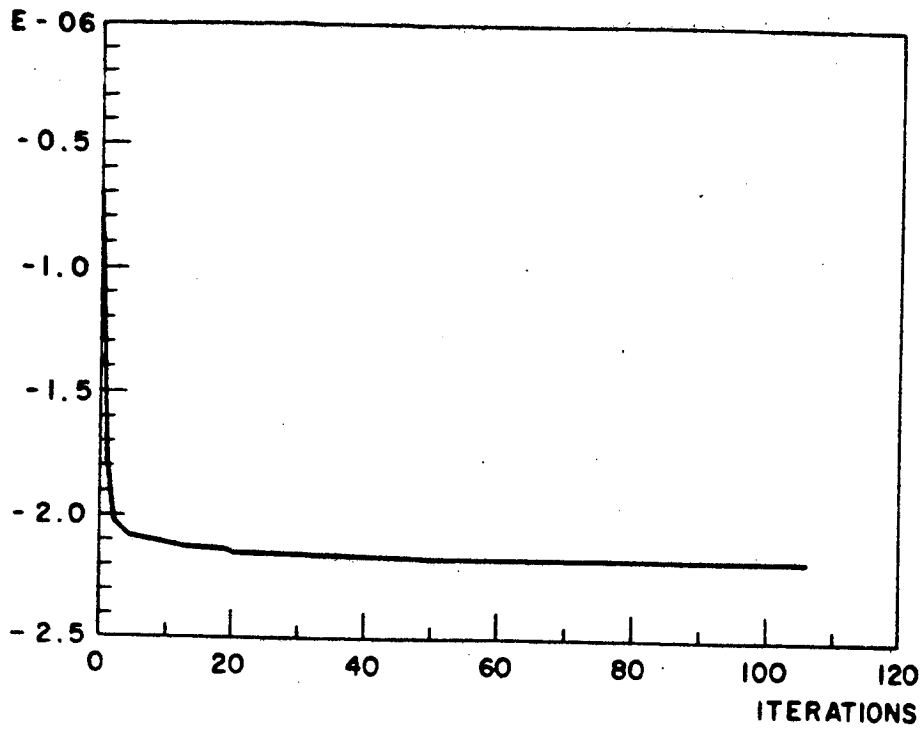


Figure 25. Example 3: Variation of the cost as a function of the number of iterations.

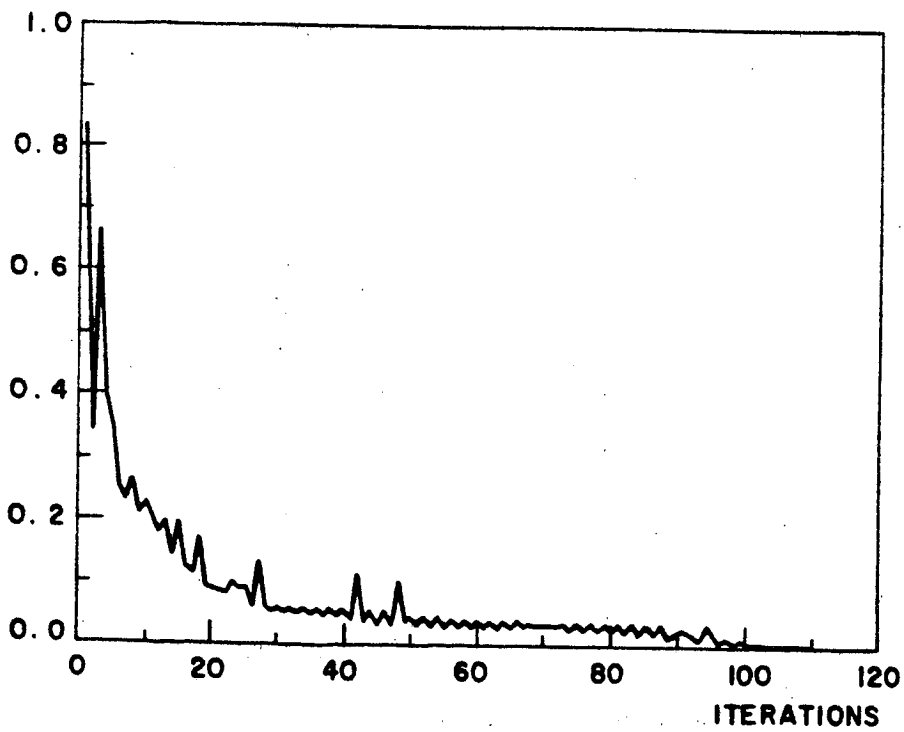


Figure 26. Example 3: Variation of the norm of the gradient.

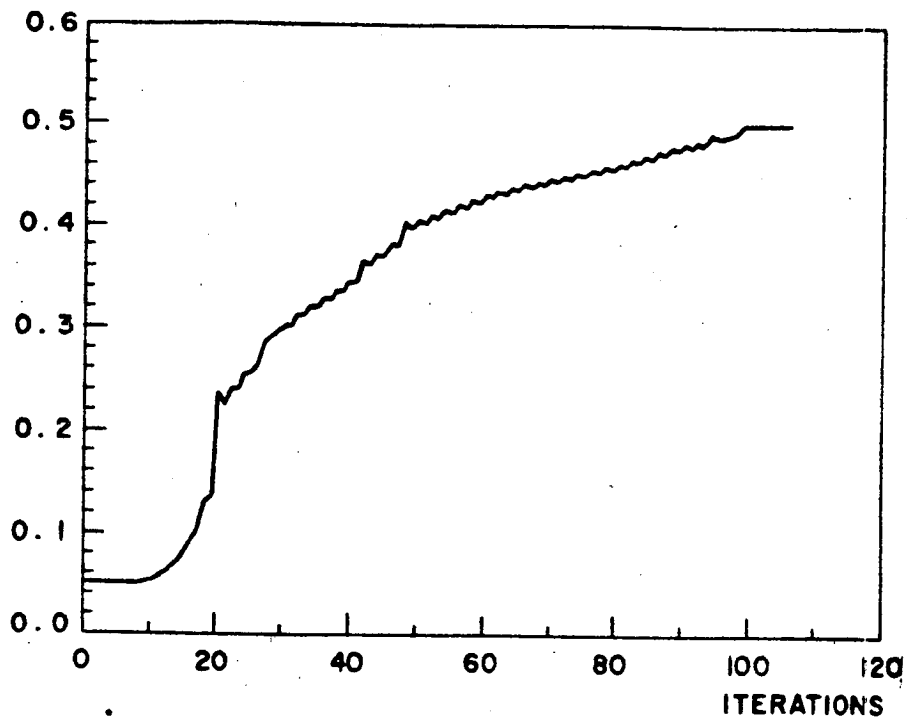


Figure 27. Example 3: Variation in the position of the sixth node as a function of the number of iterations.

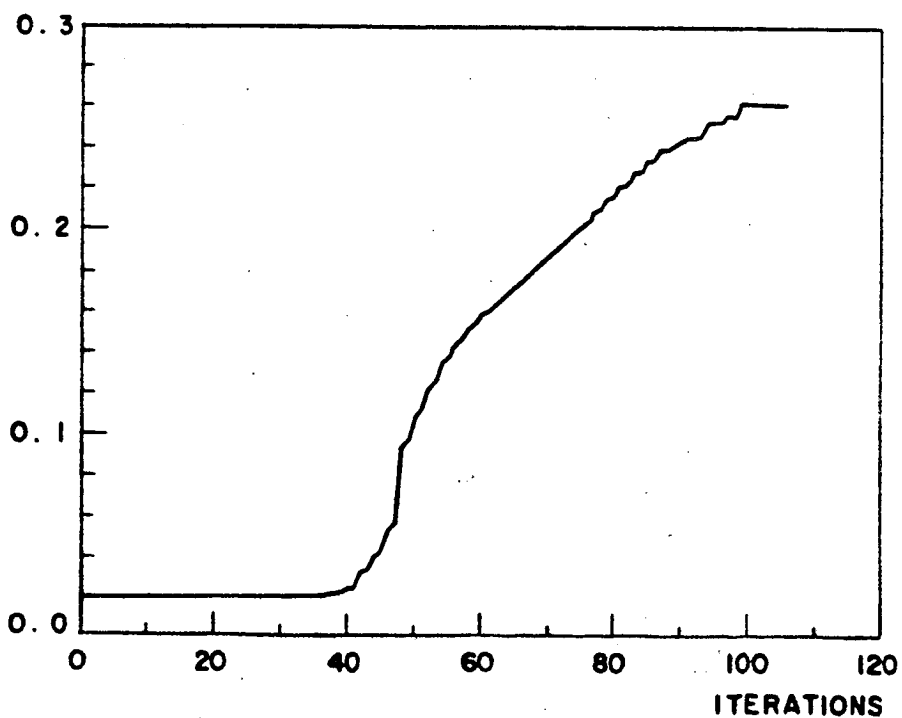


Figure 28. Example 3: Variation in the position of the second node as a function of the number of iterations.

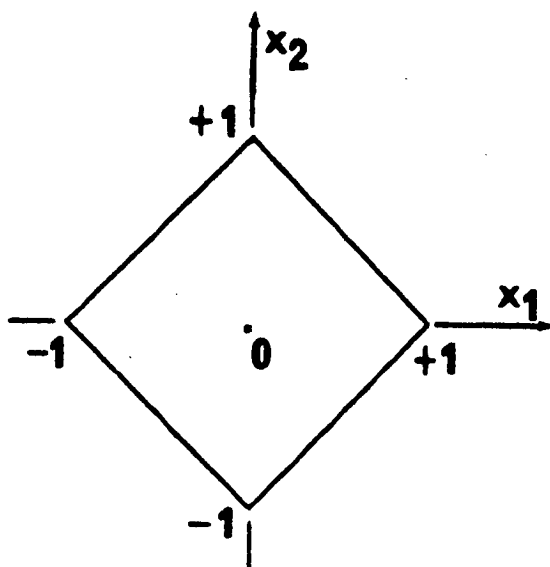


Figure 29. Domain 2.

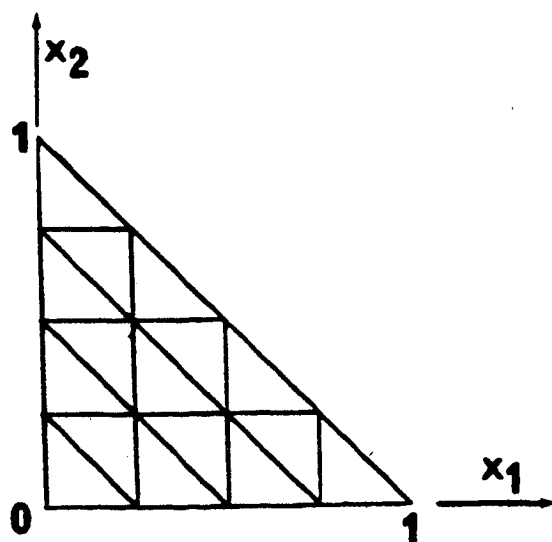


Figure 30. Initial triangulation τ_h for $n = 4$.

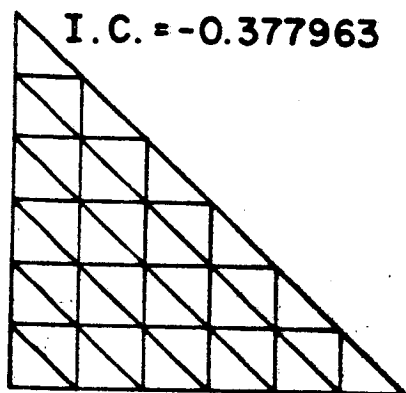


Figure 31. Initial triangulation
(I.C. = Initial Cost)

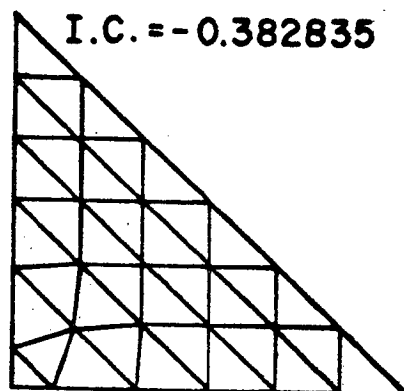


Figure 32. Second triangulation

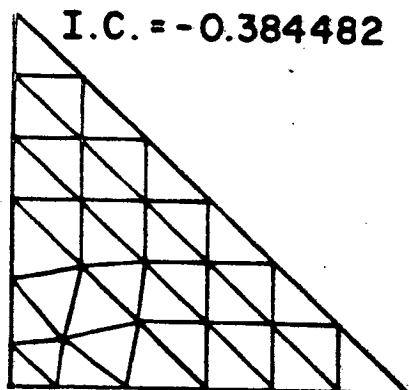


Figure 33. Third triangulation

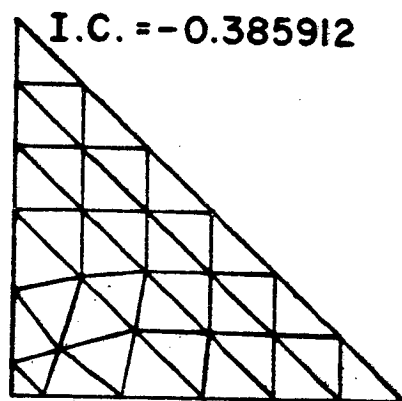


Figure 34. Fourth triangulation.

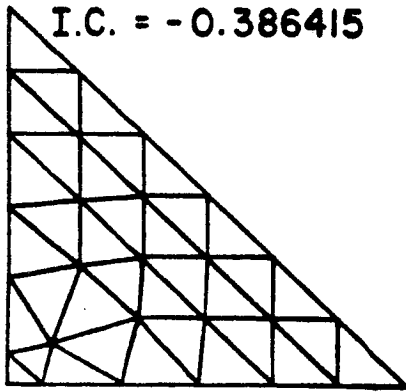


Figure 35. Fifth triangulation

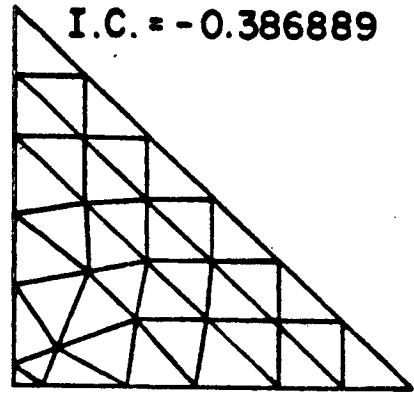


Figure 36. Sixth iteration.

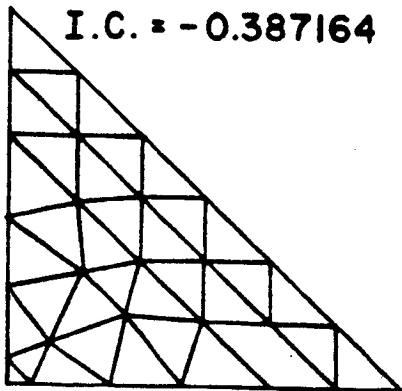


Figure 37. Eighth iteration.

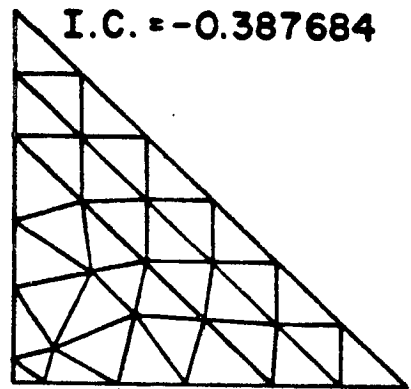


Figure 38. Ninth iteration.

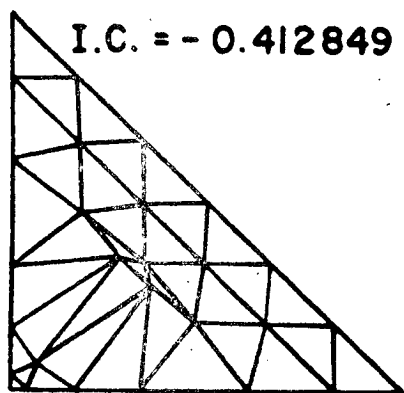


Figure 39. Tenth iteration.

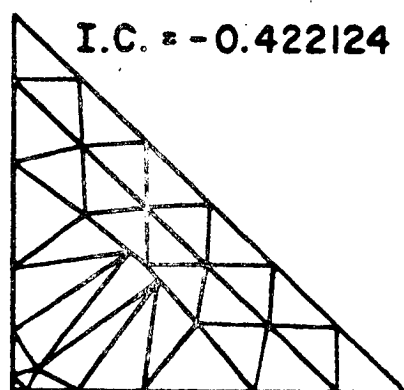


Figure 40. Eleventh iteration.

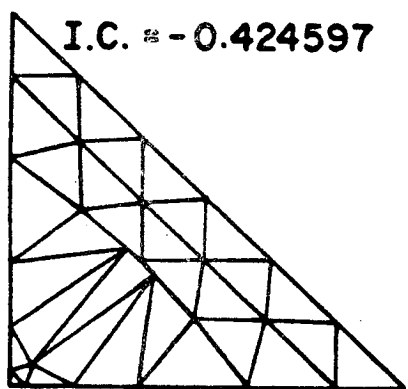


Figure 41. Twelfth iteration.

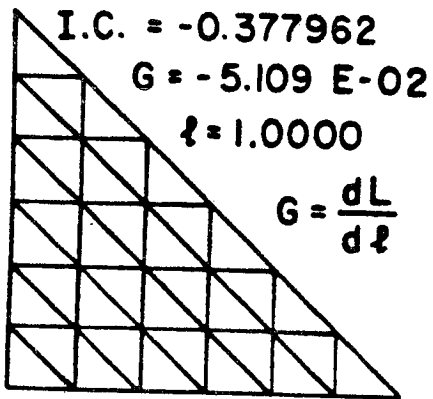


Figure 42. Initial triangulation
 (I.C. = Initial cost).

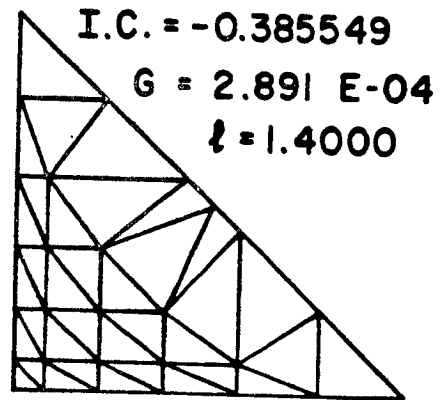


Figure 43. Second triangulation

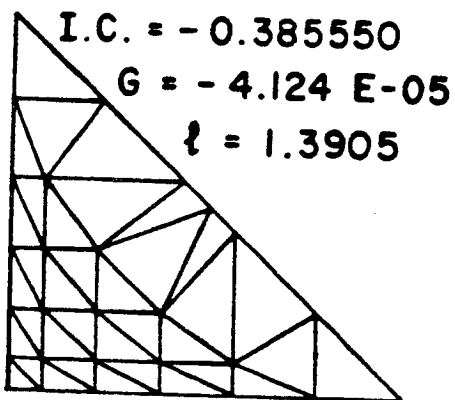


Figure 44. Third triangulation.

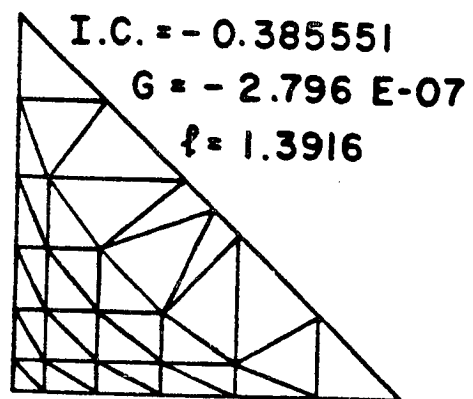


Figure 45. Fourth triangulation.

